
Hypergraph Node Classification With Graph Neural Networks

Bohan Tang¹ Zexi Liu² Keyue Jiang³ Siheng Chen^{2,4} Xiaowen Dong¹

Abstract

Hypergraphs, with hyperedges connecting more than two nodes, are key for modelling higher-order interactions in real-world data. The success of graph neural networks (GNNs) reveals the capability of neural networks to process data with pairwise interactions. This inspires the usage of neural networks for data with higher-order interactions, thereby leading to the development of hypergraph neural networks (HyperGNNs). GNNs and HyperGNNs are typically considered distinct since they are designed for data on different geometric topologies. However, in this paper, we theoretically demonstrate that, in the context of node classification, most HyperGNNs can be approximated using a GNN with a weighted clique expansion of the hypergraph. This leads to WCE-GNN, a simple and efficient framework comprising a GNN and a weighted clique expansion (WCE), for hypergraph node classification. Experiments on nine real-world hypergraph node classification benchmarks showcase that WCE-GNN demonstrates not only higher classification accuracy compared to state-of-the-art HyperGNNs, but also superior memory and runtime efficiency.

1. Introduction

Higher-order interactions involving more than two entities exist in various domains, such as co-authorships in social science (Han et al., 2009) and the spreading phenomena in epidemiology (Jhun, 2021). To model these complicated interactions, hypergraphs, an extension of traditional graphs, are widely employed (Bick et al., 2023). Hypergraphs consist of nodes representing entities and hyperedges denoting higher-order interactions that exist among multiple entities. In hypergraph machine learning, the efficient classification of nodes with the given higher-order interactions is an important problem (Agarwal et al., 2006; Antelmi et al., 2023).

The success of graph neural networks (GNNs) (Wu et al., 2020) highlights the proficiency of neural networks in processing data with pairwise interactions. Inspired by this, many hypergraph neural networks (HyperGNNs) have been proposed and widely used in the hypergraph node classification task (Feng et al., 2019; Bai et al., 2021; Huang & Yang, 2021; Chien et al., 2022; Wang et al., 2023a;b; Duta et al., 2023). These models are typically based on designs specific to hypergraphs, such as operators for learning hyperedge features (Huang & Yang, 2021; Chien et al., 2022) or hypergraph energy functions (Wang et al., 2023b). Such designs equip HyperGNNs with unique forward propagation layers. Consequently, GNNs and HyperGNNs are generally considered to be different models. This leads to little theoretical understanding of their connections in hypergraph node classification. However, such an understanding is crucial for at least three reasons: 1) it can enable the development of more efficient frameworks for processing data on hypergraphs, 2) it can provide insights into whether existing HyperGNNs fully exploit the higher-order interactions contained in hypergraphs, and 3) it can shed light on the importance of higher-order interactions for the learning task at hand.

To fill this gap, we present an original framework to reveal that a GNN with a weighted clique expansion¹ can efficiently approximate most HyperGNNs. Specifically, we provide three key theoretical results: Without non-linear activations, 1) both methods operate on the same input feature space, 2) both methods share the same inductive bias, and 3) a GNN with a weighted clique expansion can arbitrarily approximate the outputs of HyperGNNs in terms of the one-dimensional node feature approximation. With these findings, we hypothesise that a GNN with a weighted clique expansion is as powerful as existing HyperGNNs for hypergraph node classification. This leads to a simple and efficient framework for this task, called WCE-GNN, which comprises a GNN and a weighted clique expansion; see Figure 1 for an illustration. Additionally, we show that, compared with state-of-the-art HyperGNNs, WCE-GNN exhibits superior space and time efficiency.

The contributions of this work are summarised as follows:

¹A weighted clique expansion for a hypergraph is a weighted graph, wherein each weighted clique corresponds to a hyperedge in the original hypergraph. Details are in Section 2.1.

¹University of Oxford ²Shanghai Jiao Tong University
³University College London ⁴Shanghai AI Laboratory. Correspondence to: Bohan Tang <bohan.tang@eng.ox.ac.uk>.

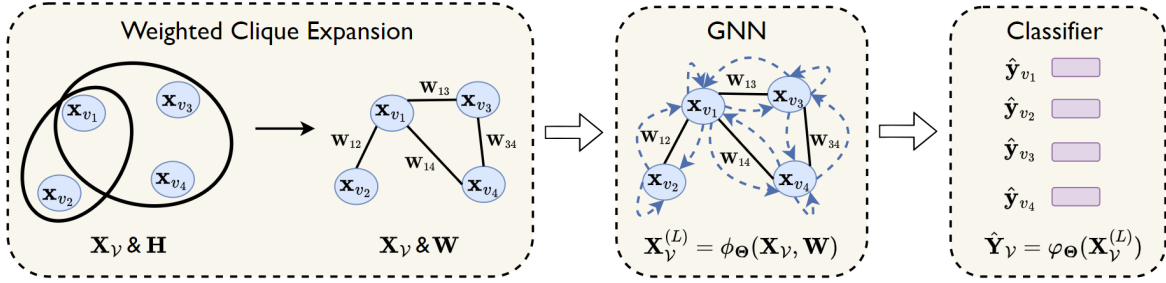


Figure 1: Overview of WCE-GNN, where \mathbf{X}_V is the given node features, \mathbf{H} is the hypergraph incidence matrix, \mathbf{W} is the adjacency matrix of the weighted clique expansion in which \mathbf{W}_{ij} is the edge weight between v_i and v_j , $\phi_{\Theta}(\cdot)$ is an L -layer GNN, $\mathbf{X}_V^{(L)}$ is the node features from $\phi_{\Theta}(\cdot)$, $\varphi_{\Theta}(\cdot)$ is a multilayer perceptron (MLP), and $\hat{\mathbf{Y}}_V$ is the node label logits.

- We introduce an original framework to analyze the connections between GNNs and HyperGNNs in the context of node classification. We demonstrate a novel theoretical result that most HyperGNNs can be well-approximated by a GNN with a weighted clique expansion. This result bridges the gap between the research in graph and hypergraph machine learning, and informs the design of an efficient framework for processing data on hypergraphs.
- We introduce WCE-GNN, a simple and efficient framework that enables the direct use of GNNs for hypergraph node classification. Furthermore, we theoretically show that the proposed WCE-GNN exhibits lower space and time complexity compared with state-of-the-art HyperGNNs.
- We conduct extensive experiments on nine real-world benchmarks. The empirical results are promising: 1) WCE-GNN shows higher classification accuracy compared with state-of-the-art HyperGNNs; 2) WCE-GNN demonstrates resilience towards the oversmoothing issue; and 3) WCE-GNN showcases superior memory and runtime efficiency.

2. Preliminary

2.1. Notation

Hypergraphs. Let $\mathcal{H} = \{\mathcal{V}, \mathcal{E}, \mathbf{H}\}$ be a hypergraph, where $\mathcal{V} = \{v_1, v_2, \dots, v_n\}$ is the node set, $\mathcal{E} = \{e_1, e_2, \dots, e_m\}$ is the hyperedge set, and $\mathbf{H} \in \{0, 1\}^{n \times m}$ is an incidence matrix in which $\mathbf{H}_{ij} = 1$ means that e_j contains node v_i and $\mathbf{H}_{ij} = 0$ otherwise. Define $\mathbf{D}_{\mathcal{H}\mathcal{V}} \in \mathbb{R}_{\geq 0}^{n \times n}$ as a diagonal matrix of node degrees and $\mathbf{D}_{\mathcal{H}\mathcal{E}} \in \mathbb{R}_{\geq 0}^{m \times m}$ as a diagonal matrix of hyperedge degrees, where $\mathbf{D}_{\mathcal{H}\mathcal{V}}^{v_i}$ and $\mathbf{D}_{\mathcal{H}\mathcal{E}}^{e_j}$ are the number of hyperedges with v_i and the number of nodes in e_j , respectively.

Weighted graphs. Let $\mathcal{G} = \{\mathcal{V}, \mathbf{W}\}$ be a weighted graph, where $\mathcal{V} = \{v_1, v_2, \dots, v_n\}$ is the node set, and $\mathbf{W} \in \mathbb{R}_{\geq 0}^{n \times n}$ is the adjacency matrix of \mathcal{G} in which $\mathbf{W}_{ij} > 0$ means that v_i and v_j are connected and $\mathbf{W}_{ij} = 0$ otherwise. We set $\mathbf{D} \in \mathbb{R}_{\geq 0}^{n \times n}$ as a diagonal node degree matrix for \mathcal{G} , where \mathbf{D}_{ii} is the sum of the i -th row of \mathbf{W} . Moreover, we denote the graph Laplacian of \mathcal{G} as $\mathbf{L} = \mathbf{D} - \mathbf{W}$.

Clique expansion. Given a hypergraph $\mathcal{H} = \{\mathcal{V}, \mathcal{E}, \mathbf{H}\}$, we define its *weighted clique expansion* as a weighted graph $\mathcal{G} = \{\mathcal{V}, \mathbf{W}\}$, where \mathcal{V} remains unchanged, and $\mathbf{W}_{ij} > 0$ if and only if v_i and v_j are connected by a hyperedge on \mathcal{H} and $\mathbf{W}_{ij} = 0$ otherwise. Hence, each hyperedge in \mathcal{H} is a clique in \mathcal{G} . Moreover, if all non-zero values in \mathbf{W} are set to 1, then \mathcal{G} reduces to an *unweighted clique expansion*.

Other notations. We denote functions or variables at the l -th layer of a neural network using the superscript (l) and use \oplus for concatenation. We use Θ to represent the learnable weight matrix in a neural network, and $\sigma(\cdot)$ for non-linear activations (e.g., ReLU and LeakyReLU).

2.2. GNNs & HyperGNNs

GNNs. Generally, GNNs learn node or graph representations by leveraging node features and the graph adjacency matrix that captures the pairwise interactions among nodes (Xu et al., 2019; Bronstein et al., 2021). Most GNNs are rooted in a neighbourhood feature aggregation paradigm, where the features of a node are iteratively updated by aggregating features of its neighbours. A seminal work is the graph convolutional network (GCN) (Kipf & Welling, 2017), whose forward propagation layer is defined as:

$$\mathbf{X}_V^{(l)} = \sigma(\mathbf{W}\mathbf{X}_V^{(l-1)}) \Theta^{(l)}, \quad (1)$$

This foundational model has inspired numerous variants (Wu et al., 2020; Bronstein et al., 2021), with enhancements such as residual connections to handle the oversmoothing issue, as exemplified by GCNII (Chen et al., 2020). A forward propagation layer in GCNII is:

$$\mathbf{X}_V^{(l)} = \sigma\left(\left((1 - \epsilon_l)\mathbf{W}\mathbf{X}_V^{(l-1)} + \epsilon_l\mathbf{X}_V^{(0)}\right)\left((1 - \epsilon'_l)\mathbf{I}_d + \epsilon'_l\Theta^{(l)}\right)\right), \quad (2)$$

where $\epsilon_l, \epsilon'_l \in \mathbb{R}$ are two hyperparameters, and $\mathbf{I}_d \in \mathbb{R}^{d \times d}$ is an identity matrix. Notably, setting $\epsilon_l = 0$ and $\epsilon'_l = 1$ in Eq. (2) reverts it to Eq. (1). In the following, our discussion on GNNs primarily utilises the formation in Eq. (2).

HyperGNNs. Typically, HyperGNNs process data on hypergraphs by utilizing node features and the hypergraph incidence matrix that captures higher-order interactions among nodes. A seminal work (Chien et al., 2022) demonstrates

that most HyperGNNs (Feng et al., 2019; Yadati et al., 2019; Dong et al., 2020; Huang & Yang, 2021; Bai et al., 2021) employ a two-step message passing mechanism: node features are first aggregated to hyperedges to generate hyperedge features, which are aggregated back to nodes to update node features, which can be formulated as:

$$\begin{aligned}\mathbf{X}_{\mathcal{E}}^{(l)} &= f_{\mathcal{V} \rightarrow \mathcal{E}}(\mathbf{X}_{\mathcal{V}}^{(l-1)}, \mathbf{X}_{\mathcal{E}}^{(l-1)}), \\ \mathbf{X}_{\mathcal{V}}^{(l)} &= f_{\mathcal{E} \rightarrow \mathcal{V}}(\mathbf{X}_{\mathcal{V}}^{(l-1)}, \mathbf{X}_{\mathcal{E}}^{(l)}),\end{aligned}$$

where $\mathbf{X}_{\mathcal{E}} \in \mathbb{R}^{m \times d}$ denotes the hyperedge features, and $f_{\mathcal{V} \rightarrow \mathcal{E}}(\cdot)$ and $f_{\mathcal{E} \rightarrow \mathcal{V}}(\cdot)$ are two feature aggregation functions. More recent developments include models by Wang et al.(2023a) and Wang et al.(2023b). Wang et al.(2023a) design the model from a hypergraph diffusion perspective, while Wang et al.(2023b) unroll an optimisation algorithm minimising an hypergraph energy function. In the following, we concentrate on five state-of-the-art HyperGNNs: UniGNN (Huang & Yang, 2021), AllDeepSets (Chien et al., 2022), AllSetTransformer (Chien et al., 2022), ED-HNN (Wang et al., 2023a), and PhenomNN (Wang et al., 2023b). More details of them are in Appendix B.

2.3. Problem Formulation

Hypergraph node classification. Let node features be $\mathbf{X}_{\mathcal{V}} = [\mathbf{x}_{v_1}^{\top}, \mathbf{x}_{v_2}^{\top}, \dots, \mathbf{x}_{v_n}^{\top}]^{\top} \in \mathbb{R}^{n \times d}$, which is a matrix that contains d -dimensional features, \mathcal{V}_{lab} be the set of labelled nodes with ground truth labels $\mathbf{Y}_{lab} = \{\mathbf{y}_v\}_{v \in \mathcal{V}_{lab}}$, where $\mathbf{y}_{v_i} \in \{0, 1\}^c$ be a one-hot label, and $\mathcal{V}_{un} = \mathcal{V} \setminus \mathcal{V}_{lab}$ be a set of unlabeled nodes. The hypergraph node classification task requires a model to classify nodes within \mathcal{V}_{un} based on $\mathbf{X}_{\mathcal{V}}$, known labels \mathbf{Y}_{lab} , and the given hypergraph structure \mathbf{H} . In subsequent sections, we assume the hypergraph does not have isolated nodes or empty/duplicate hyperedges, and all the node features are d -dimensional unless otherwise noted.

3. Theoretical Analyses

We analyse the connections between the GNNs and HyperGNNs in terms of three critical node-level properties: 1) the input feature space utilized by HyperGNNs/GNNs/ for the node feature update, 2) the inductive bias inherent in HyperGNNs/GNNs for the node feature generation, and 3) the expressive power of HyperGNNs/GNNs for the node feature approximation. Based on our analysis, we propose a **GNN Effectiveness Hypothesis**.

3.1. Input Feature Space

We summarise the connections between GNNs and HyperGNNs in terms of the input feature space as Proposition 3.1.

Proposition 3.1. *Let $\mathcal{H} = \{\mathcal{V}, \mathcal{E}, \mathbf{H}\}$ denote a hypergraph and $\mathcal{G} = \{\mathcal{V}, \mathbf{W}\}$ be its weighted clique expansion. For any node $v_i \in \mathcal{V}$, let $\mathcal{X}_{\mathcal{H}^l}^I$ and $\mathcal{X}_{\mathcal{G}^l}^I$ denote the input feature*

space for the l -th layer of HyperGNNs on \mathcal{H} and GNNs on \mathcal{G} , respectively, used in updating the features of node v_i . Assume that GNNs and HyperGNNs operate without non-linear activations. Then, $\mathcal{X}_{\mathcal{H}^l}^I = \mathcal{X}_{\mathcal{G}^l}^I$.

Proof Sketch. To prove this proposition, we first demonstrate that, without non-linear activation, the forward propagation layers in HyperGNNs on \mathcal{H} and GNNs on \mathcal{G} can be reformulated as special cases of the following formula:

$$\mathbf{x}_{v_i}^{(l)} = f_0(\mathbf{x}_{v_i}^{(l-1)}) + \rho f_1(\mathbf{x}_{v_i}^{(0)}) + \sum_{v_j \in \mathcal{N}_{\mathcal{G}^l} v_i} f_2(\mathbf{x}_{v_j}^{(l-1)}), \quad (3)$$

where $f_0(\cdot)$, $f_1(\cdot)$ and $f_2(\cdot)$ represent three parameterised functions, $\mathcal{N}_{\mathcal{G}^l} v_i$ is the set of neighbours of v_i on \mathcal{G} , and hyperparameter $\rho \in \mathbb{R}$ controls the use of initial residual connections in the model, with $\rho = 0$ indicating no usage. Based on Eq.(3), when a HyperGNN/GNN incorporates the initial residual connection, $\mathcal{X}_{\mathcal{H}^l}^I = \mathcal{X}_{\mathcal{G}^l}^I = \{\mathbf{x}_{v_i}^{(l-1)}, \mathbf{x}_{v_i}^{(0)}, \oplus_{v_j \in \mathcal{N}_{\mathcal{G}^l} v_i} \mathbf{x}_{v_j}^{(l-1)}\}$. In contrast, when a HyperGNN/GNN is implemented without initial residual connections, $\mathcal{X}_{\mathcal{H}^l}^I = \mathcal{X}_{\mathcal{G}^l}^I = \{\mathbf{x}_{v_i}^{(l-1)}, \oplus_{v_j \in \mathcal{N}_{\mathcal{G}^l} v_i} \mathbf{x}_{v_j}^{(l-1)}\}$. The detailed proof is provided in Appendix D. \square

This proposition demonstrates that, despite there are differences in the original input formations of models, namely, a GNN utilising the pairwise interactions within nodes captured by a weighted clique expansion and HyperGNNs using higher-order interactions among nodes embedded in a hypergraph, both models operate on the same input feature space to update node features.

3.2. Inductive Bias

To connect GNNs and HyperGNNs in terms of their inductive bias, we first introduce the following definition:

Definition 3.1 (hypergraph smooth feature space). Given a hypergraph $\mathcal{H} = \{\mathcal{V}, \mathcal{E}, \mathbf{H}\}$ with initial node features $\mathbf{X}_{\mathcal{V}}^{(0)} \in \mathbb{R}^{n \times d}$, the hypergraph smooth feature space $\mathcal{X}^S \subset \mathbb{R}^{n \times d}$ is defined such that for any $\mathbf{X} \in \mathcal{X}^S$, there exists a weighted clique expansion $\mathcal{G} = \{\mathcal{V}, \mathbf{W}\}$ of \mathcal{H} satisfying:

$$\mathbf{X} = \arg \min_{\mathbf{X}'} \text{tr}(\mathbf{X}'^{\top} \mathbf{L} \mathbf{X}') + \rho \text{tr}[(\mathbf{X}' - \mathbf{S} \mathbf{X}_{\mathcal{V}}^{(0)})^{\top} \mathbf{P} (\mathbf{X}' - \mathbf{S} \mathbf{X}_{\mathcal{V}}^{(0)})], \quad (4)$$

where $\mathbf{L} \in \mathbb{R}^{n \times n}$ is the graph Laplacian matrix of \mathcal{G} , $\mathbf{S}, \mathbf{P} \in \mathbb{R}_{\geq 0}^{n \times n}$ are diagonal matrices, and $\rho \in \mathbb{R}_{\geq 0}$ is a regularisation parameter.

Accordingly, we establish the connections between GNNs and HyperGNNs with respect to the inductive bias as:

Proposition 3.2. *Let $\mathcal{H} = \{\mathcal{V}, \mathcal{E}, \mathbf{H}\}$ denote a hypergraph and $\mathcal{G} = \{\mathcal{V}, \mathbf{W}\}$ be its weighted clique expansion. Define $\mathbf{X}_{\mathcal{H}^L}^{(L)} \in \mathbb{R}^{n \times d}$ as the output of an L -layer HyperGNN on \mathcal{H} , and $\mathbf{X}_{\mathcal{G}^L}^{(L)} \in \mathbb{R}^{n \times d}$ as the output of an L -layer GNN on \mathcal{G} . Assume that: 1) L approaches infinity, i.e. $L \rightarrow$*

$+\infty$; and 2) The HyperGNN/GNN on \mathcal{H}/\mathcal{G} with the non-linear activation removed and the learnable parameters fixed. Then, $\mathbf{X}_{\mathcal{H}_v}^{(L)}, \mathbf{X}_{\mathcal{G}_v}^{(L)} \in \mathcal{X}^S$.

Proof Sketch. We focus on GNNs and HyperGNNs with non-linear activation removed and learnable parameters fixed. Firstly, we determine \mathbf{X}_0^* and \mathbf{X}_1^* that minimise the right-hand side of Eq. (4) with $\rho = 0$ and $\rho > 0$, respectively. Furthermore, we demonstrate that, without the initial residual connection, the output of a HyperGNN/GNN on \mathcal{H}/\mathcal{G} converges to \mathbf{X}_0^* as $L \rightarrow +\infty$; and, with the initial residual connection, the output of a HyperGNN/GNN on \mathcal{H}/\mathcal{G} converges to \mathbf{X}_1^* as $L \rightarrow +\infty$. Details are in appendix E. \square

Notably, minimising the first term in the right-hand side of Eq. (4) enhances feature similarity among connected nodes on \mathcal{G} , and minimising the second term encourages the generated node features to retain the information from the initial node features. Hence, this proposition shows that, while GNNs on \mathcal{G} and HyperGNNs on \mathcal{H} take different topological structures as input, they share the same inductive bias for the node feature generation. Specifically, they promote similarity in features among neighbouring nodes on a weighted clique expansion while potentially maintaining the information from the initial features of these nodes.

3.3. Expressive Power

Before exploring the expressivity connections between GNNs and HyperGNNs, we make an assumption:

Assumption 3.1. Let $\mathcal{X}_{\mathcal{H}_{1d}}^O$ denote the output space of HyperGNNs in terms of generating one-dimensional node features for n nodes. We assume that $\mathcal{X}_{\mathcal{H}_{1d}}^O \subseteq \mathbb{R}^n$.

Drawing inspiration from the research in spectral GNNs (Wang & Zhang, 2022), we link the expressive power of GNNs and HyperGNNs in Proposition 3.3.

Proposition 3.3. Let $\mathcal{H} = \{\mathcal{V}, \mathcal{E}, \mathbf{H}\}$ denote a hypergraph, and $\mathcal{G} = \{\mathcal{V}, \mathbf{W}\}$ be its weighted clique expansion. Define $\mathbf{X}_{\mathcal{V}}^{(0)} \in \mathbb{R}^{n \times d}$ as the initial node features and $g_{\Theta_L}(\cdot)$ as an L -layer GNN without non-linear activations, parameterised by $\Theta_L = [\Theta^{(1)}, \dots, \Theta^{(L)}]$. Assume that: 1) the GNN includes the initial residual connection, 2) all rows of $\mathbf{U}^\top \mathbf{X}_{\mathcal{V}}^{(0)}$ are not zero vectors with $\mathbf{U} \in \mathbb{R}^{n \times n}$ comprising the linearly independent eigenvectors of \mathbf{W} , and 3) \mathbf{W} has no repeated eigenvalues. For any $\mathbf{X}_{\mathcal{H}_v} \in \mathcal{X}_{\mathcal{H}_{1d}}^O$ generated by a HyperGNN on \mathcal{H} , there exists Θ_L^* such that $g_{\Theta_L^*}(\mathbf{X}_{\mathcal{V}}^{(0)}, \mathbf{W}) = \mathbf{X}_{\mathcal{H}_v}$.

Proof Sketch. Firstly, we reformulate the one-dimensional output of an L -layer GNN with the initial residual connection as $\mathbf{X}_{\mathcal{V}}^{(L)} = \sum_{l=0}^L \theta_l \mathbf{W}^l \mathbf{X}_{\mathcal{V}}^{(0)} \Theta$, where $\Theta \in \mathbb{R}^d$ denotes learnable parameters, and $\theta_l \in \mathbb{R}$ denotes a learnable parameter. Next, inspired by Theorem 4.1 in Wang & Zhang

(2022), we show that there exists $[\theta_0^*, \dots, \theta_L^*]$ and $\Theta^* \in \mathbb{R}^d$, for any $\mathbf{X}_{\mathcal{H}_v} \in \mathcal{X}_{\mathcal{H}_{1d}}^O$, such that $\mathbf{X}_{\mathcal{H}_v} = \sum_{l=0}^L \theta_l^* \mathbf{W}^l \mathbf{X}_{\mathcal{V}}^{(0)} \Theta^*$ under the conditions 2) and 3) in Proposition 3.3. The detailed proof can be found in Appendix F. \square

This proposition indicates that, in terms of the one-dimensional node feature approximation, GNNs on \mathcal{G} are as expressive as HyperGNNs on \mathcal{H} .

3.4. GNN Effectiveness Hypothesis

Building on the preceding discussions, we propose the following hypothesis on the effectiveness of GNNs:

Hypothesis 3.1. A GNN with a weighted clique expansion is as powerful as existing HyperGNNs for classifying nodes on hypergraphs.

Thereon, we propose an alternative to HyperGNNs, a framework called WCE-GNN, in the next section. We empirically examine Hypothesis 3.1 based on WCE-GNN in Section 6.2.

4. Practical Learning Framework: WCE-GNN

General formulation. We summarise the application of a GNN with a weighted clique expansion for hypergraph node classification into two primary steps. First, implement the forward propagation layer using a suitable GNN architecture. Second, design a strategy to assign appropriate weights to edges in the weighted clique expansion.

Model design. With the general formulation, we first implement the forward propagation in our WCE-GNN using the architecture of GCNII (Chen et al., 2020), which is introduced in Section 2.2. Thus, the forward propagation layer of our model is defined as Eq. (2). The intuition behind the choice of GCNII is that it is a simple and efficient GNN architecture with the initial residual connection (Chen et al., 2020; Wu et al., 2020). We present a discussion on the crucial role of the initial residual connection in GNNs for hypergraph node classification in Appendix G. After having the forward propagation layer, we generate the edge weights in the weighted clique expansion as follows:

$$\mathbf{W}_{H_{ij}} = \sum_{k=1}^m \frac{\delta(v_i, v_j, e_k)}{\mathbf{D}_{\mathcal{H}_{kk}}^\varepsilon}, \quad (5)$$

where $\delta(\cdot)$ is a function that returns 1 if e_k connect v_i and v_j and returns 0 otherwise. In Appendix H, we show that, under certain conditions, the value of $\mathbf{W}_{H_{ij}}$ is positively correlated with the probability of nodes v_i and v_j having the same label. This property makes the weighted clique expansion fit the homophily assumption, which is that connected nodes tend to be similar to each other (McPherson et al., 2001). Following the GNN literature (Wu et al., 2020), we

Table 1: Complexity of our method and HyperGNNs. Here, n is the number of nodes, m is the number of hyperedges, m' is the number of edges in the clique expansion, $\|\mathbf{H}\|_0$ is the number of non-zero entities in \mathbf{H} , L is the number of layers, P is the number of layers of the MLP in each layer, h is the number of attention heads, and d is the feature dimension.

	WCE-GNN (Ours)	UniGNN	AllDeepSets	AllSetTransformer	ED-HNN	PhenomNN
Space Complexity	$\mathcal{O}(Lnd + Ld^2)$	$\mathcal{O}(L(n+m)d + Ld^2)$	$\mathcal{O}(L(n+m)d + Ld^2)$	$\mathcal{O}(L(n+m+h)d + Ld^2)$	$\mathcal{O}(L(n+m)d + Ld^2)$	$\mathcal{O}(Lnd + Ld^2)$
Time Complexity	$\mathcal{O}(Lm'd + Lnd^2)$	$\mathcal{O}(L(n+m + \ \mathbf{H}\ _0)d + Lnd^2)$	$\mathcal{O}(LP\ \mathbf{H}\ _0d + LP(n+m)d^2)$	$\mathcal{O}(Lh(n+m + \ \mathbf{H}\ _0)d^2 + LP(n+m)d^2)$	$\mathcal{O}(L\ \mathbf{H}\ _0d + LP(n+m)d^2)$	$\mathcal{O}(Lm'd + Lnd^2)$

add self-loops to \mathbf{W}_H and symmetrically normalised it by:

$$\hat{\mathbf{W}}_H = \tilde{\mathbf{D}}_H^{-1/2} \tilde{\mathbf{W}}_H \tilde{\mathbf{D}}_H^{-1/2}. \quad (6)$$

where $\tilde{\mathbf{W}}_H = \mathbf{W}_H + \mathbf{I}_n$ and $\tilde{\mathbf{D}}_H \in \mathbb{R}^{n \times n}$ is the diagonal node degree matrix corresponding to $\tilde{\mathbf{W}}_H$.

Training & inference. To generate node labels, we send the output of an L -layer WCE-GNN into an MLP:

$$\hat{\mathbf{Y}}_{\mathcal{V}} = \text{MLP}_{\Theta^{(C)}}(\mathbf{X}_{\mathcal{V}}^{(L)}), \quad (7)$$

where $\hat{\mathbf{Y}}_{\mathcal{V}} \in (0, 1)^{n \times c}$ denotes the node label logits, and $\text{MLP}_{\Theta^{(C)}}$ denotes an MLP parameterised by $\Theta^{(C)}$. The model is trained by the cross-entropy loss function:

$$\mathcal{L}(\mathbf{Y}_{lab}, \hat{\mathbf{Y}}_{\mathcal{V}}) = -\frac{1}{|\mathcal{V}_{lab}|} \sum_{v_i \in \mathcal{V}_{lab}} \mathbf{y}_{v_i} \log(\hat{\mathbf{y}}_{v_i}^{\top}), \quad (8)$$

where $\log(\cdot)$ is an element-wise logarithmic function. Our WCE-GNN is summarised in Algorithm 1.

Computational efficiency. We summarise the space and time complexity of our WCE-GNN and five representative HyperGNNs in Table 1. For the space complexity, two critical elements demand consideration: features, which include both the input and generated features, and the input structure. We focus on the space required by features for two reasons: 1) Features cannot be stored sparsely like the input structure; and 2) Space requirements for the generated features increase with the number of layers, while those for the input structure remain constant. According to Table 1, our method has the lowest space complexity compared to others. For the time complexity, our focus is on the computations performed by each forward propagation layer. These computations significantly contribute to the overall runtime as they cannot be executed during the pre-processing stage. Referring to Table 1, although the values of m' , m , P , and $\|\mathbf{H}\|_0$ may vary with the dataset and the model, it is clear that the time complexity of these methods is of the same order, increasing linearly with L . Notably, while sharing the same big O notation for complexity with our method, the forward propagation layer of PhenomNN requires computing more intermediate results, making it more computationally intensive in practice than our method. We empirically study the computational efficiency in Section 6.2.

5. Related Work

Hypergraph node classification. There are two predominant hypergraph node classification approaches: traditional and deep-learning-based methods. Traditional meth-

Algorithm 1 WCE-GNN

*/*Training*/*

Input: $\mathbf{X}_{\mathcal{V}}$, $\mathbf{Y}_{\mathcal{V}}$, \mathcal{H} , \mathcal{V}_{lab} , the number of layers L , the number of the training iterations T .

Output: The optimal model parameters $[\Theta^{(1)*}, \dots, \Theta^{(L)*}, \Theta^{(C)*}]$.

Randomly initialise $[\Theta^{(1)}, \dots, \Theta^{(L)}, \Theta^{(C)}]$, set $\mathbf{X}_{\mathcal{V}}^{(0)}$ as

$\mathbf{X}_{\mathcal{V}}$, generate $\hat{\mathbf{W}}_H$ by Eq. (5) and (6).

for $t = 1 : T$ **do**

for $l = 1 : L$ **do**

 | Update the node features by Eq. (2).

end

 Generate the node label logits $\hat{\mathbf{Y}}_{\mathcal{V}}$ by Eq. (7).

 Update $[\Theta^{(0)}, \dots, \Theta^{(L)}, \Theta^{(C)}]$ by minimising Eq. (8) with the gradient descent.

end

*/*Inference*/*

Input: $\mathbf{X}_{\mathcal{V}}$ and $[\Theta^{(1)*}, \dots, \Theta^{(L)*}, \Theta^{(C)*}]$.

Output: Predicted node label logits $\hat{\mathbf{Y}}_{\mathcal{V}}$.

Set $\mathbf{X}_{\mathcal{V}}^{(0)}$ as $\mathbf{X}_{\mathcal{V}}$, and generate $\hat{\mathbf{W}}_H$ by Eq. (5) and Eq. (6).

for $l = 1 : L$ **do**

 | Update the node features by Eq. (2).

end

Generate the label logits $\hat{\mathbf{Y}}_{\mathcal{V}}$ by Eq. (7).

ods (Bolla, 1993; Gibson et al., 2000; Zhou et al., 2005a; Agarwal et al., 2006) primarily focus on extending the graph Laplacian matrix (Mohar et al., 1991; Grone & Merris, 1994; Zhou et al., 2005b) to formulate a hypergraph Laplacian matrix. With the eigenvectors derived from the specially designed matrix, the hypergraph node classification task can be solved in two steps: 1) The eigenvectors are utilised as inputs by a clustering algorithm that separates nodes into distinct clusters; and 2) Unlabeled nodes in each cluster are assigned labels based on the most common labels in the cluster. Most deep-learning-based methods (Feng et al., 2019; Bai et al., 2021; Huang & Yang, 2021; Chien et al., 2022; Wang et al., 2023a;b) develop HyperGNNs through adjusting the designs of existing GNNs (Kipf & Welling, 2017; Bodnar et al., 2022; Atwood & Towsley, 2016; Gilmer et al., 2017; Xu et al., 2019; Chen et al., 2021; Yang et al., 2021) to classify nodes in an end-to-end paradigm.

Although the aforementioned hypergraph learning approaches are methodologically grounded in the research

Table 2: Dataset statistics. CE homophily is the homophily score based on clique expansions of hypergraphs; details of this score can be found in Appendix I.

	Cora	Citeseer	Pubmed	Cora-CA	DBLP-CA	Congress	Senate	Walmart	House
# nodes	2708	3312	19717	2708	41302	1718	282	88860	1290
# hyperedges	1579	1079	7963	1072	22363	83105	315	69906	340
# features	1433	3703	500	1433	1425	100	100	100	100
# classes	7	6	3	7	6	2	2	11	2
CE homophily	0.897	0.893	0.952	0.803	0.869	0.555	0.498	0.530	0.509

Table 3: Classification accuracy (%) for baselines and our method on benchmarks. The state-of-the-art result on each dataset is highlighted in **bold font**. “-” indicates that no results were reported in previous papers, and no open-source code is available for this method.

	Cora	Citeseer	Pubmed	Cora-CA	DBLP-CA	Congress	Senate	Walmart	House
HGNN	79.39 ± 1.36	72.45 ± 1.16	86.44 ± 0.44	82.64 ± 1.65	91.03 ± 0.20	91.26 ± 1.15	48.59 ± 4.52	62.00 ± 0.24	61.39 ± 2.96
HCHA	79.14 ± 1.02	72.42 ± 1.42	86.41 ± 0.36	82.55 ± 0.97	90.92 ± 0.22	90.43 ± 1.20	48.62 ± 4.41	62.35 ± 0.26	61.36 ± 2.53
UniGNN	78.81 ± 1.05	73.05 ± 2.21	88.25 ± 0.40	83.60 ± 1.14	91.69 ± 0.19	94.81 ± 0.81	49.30 ± 4.25	54.45 ± 0.37	67.25 ± 2.57
AllDeepSets	76.88 ± 1.80	70.83 ± 1.63	88.75 ± 0.33	81.97 ± 1.50	91.27 ± 0.27	91.80 ± 1.53	48.17 ± 5.67	64.55 ± 0.33	67.82 ± 2.40
AllSetTransformer	78.58 ± 1.47	73.08 ± 1.20	88.72 ± 0.37	83.63 ± 1.47	91.53 ± 0.23	92.16 ± 1.05	51.83 ± 5.22	65.46 ± 0.25	69.33 ± 2.20
ED-HNN	80.31 ± 1.35	73.70 ± 1.38	89.03 ± 0.53	83.97 ± 1.55	91.90 ± 0.19	95.00 ± 0.99	64.79 ± 5.14	66.91 ± 0.41	72.45 ± 2.28
PhenomNN	82.29 ± 1.42	75.10 ± 1.59	88.07 ± 0.48	85.81 ± 0.90	91.91 ± 0.21	88.24 ± 1.47	67.70 ± 5.24	62.98 ± 1.36	70.71 ± 2.35
SheafHyperGNN	81.30 ± 1.70	74.71 ± 1.23	87.68 ± 0.60	85.52 ± 1.28	91.59 ± 0.24	91.81 ± 1.60	68.73 ± 4.68	-	73.84 ± 2.30
WCE-GNN (ours)	82.35 ± 1.28	74.73 ± 1.45	88.64 ± 0.31	86.25 ± 1.25	92.16 ± 0.29	95.16 ± 1.03	70.00 ± 4.93	68.92 ± 0.38	75.73 ± 1.69

of graph machine learning, there is a notable gap in the theoretical exploration of the connections between graph and hypergraph machine learning research. In this paper, we aim to bridge this gap. Notably, while there are some previous works are analogous to directly applying GNNs with a clique/star-shape expansion to the hypergraph node classification task (Feng et al., 2019; Bai et al., 2021; Huang & Yang, 2021), these works only use the convolution operator in GNNs intuitively without studying the theoretical connections between GNNs and HyperGNNs. To our knowledge, the work most related to ours is that of Agarwal et al. (2006), which establishes the connection between traditional graph and hypergraph machine learning approaches. They show that most hypergraph Laplacian matrices can be represented as graph Laplacian matrices of weighted clique expansions of the hypergraphs. Our research differs by focusing on the connection of deep-learning-based methods, showing that most existing HyperGNNs can be well-approximated by a GNN equipped with a weighted clique expansion.

6. Experiments

6.1. Experiment Setup

Datasets. We use nine publicly available datasets, including five homophilic hypergraphs (Cora, Citeseer, Pubmed, Cora-CA, and DBLP-CA) from Yadati et al. (2019), and four heterophilic hypergraphs (Congress, Senate, Walmart and House) from Wang et al. (2023a). The details of these datasets are summarised in Table 2.

Baselines. We compare WCE-GNN with eight state-of-

the-art HyperGNNs for hypergraph node classification: HGNN (Feng et al., 2019), HCHA (Bai et al., 2021), UniGNN (Huang & Yang, 2021), AllDeepSets (Chien et al., 2022), AllSetTransformer (Chien et al., 2022), ED-HNN (Wang et al., 2023a), PhenomNN (Wang et al., 2023b), and SheafHyperGNN (Duta et al., 2023).

Metrics. Following prior research (Feng et al., 2019; Bai et al., 2021; Huang & Yang, 2021; Chien et al., 2022; Wang et al., 2023a;b; Duta et al., 2023), we evaluate baselines and our method by accuracy (%), which is defined as the ratio between the number of correct predictions to the total number of predictions. We show the results of the average accuracy and the associated std in ten different runs.

Implementation details. Following previous works (Feng et al., 2019; Yadati et al., 2019; Bai et al., 2021; Huang & Yang, 2021; Chien et al., 2022; Wang et al., 2023a;b; Duta et al., 2023), we randomly partition the dataset into training, validation, and test sets using a 50%/25%/25% split. All experiments were performed on an RTX 3090 using PyTorch. Our code is available at: <https://github.com/tbh-98/WCE-GNN>.

6.2. Results & Analysis

Classification accuracy. Table 3 summarises the classification accuracy comparison between the proposed WCE-GNN and baseline methods. This table demonstrates that WCE-GNN outperforms all the baselines in seven of the nine datasets. These results empirically support the GNN Effectiveness Hypothesis shown in Section 3.4, namely, a GNN with a weighted clique expansion is as powerful as

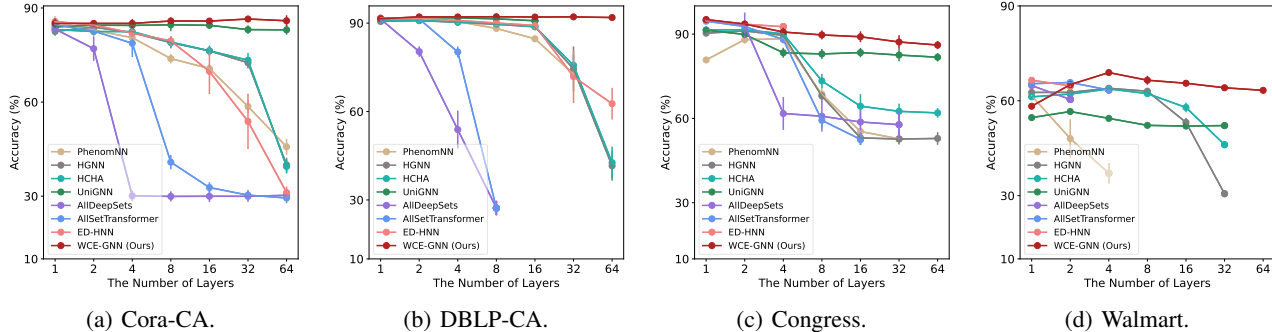


Figure 2: The impact of the number of model layers on the accuracy. Notably, some models experience an Out Of Memory (OOM) issue when the layer count reaches a certain threshold, and we only report available results for such models.

HyperGNNs for hypergraph node classification.

Impacts from the number of model layers.² We study the impacts of the number of model layers on the model performance from two main perspectives: 1) the classification accuracy, and 2) the computational efficiency.

For the classification accuracy, given that our method is based on the GNN architecture, it would be important to test its resilience against the oversmoothing issue (Li et al., 2018; Rusch et al., 2023). This issue refers to the tendency of a GNN model to produce indistinguishable features for nodes in different classes as the model depth increases. Figure 2 illustrates how the classification accuracy of our model and the baselines varies with the increase in the number of model layers. Compared with baseline models, our model maintains consistent accuracy as the layers deepen. Moreover, the results in Figure 2(a), 2(b), and 2(d) suggest that increasing the depth of our model appropriately can improve its classification accuracy. These results demonstrate the robustness of our WCE-GNN against the oversmoothing issue. We contribute this robustness to the usage of the residual connections in the GCNII architecture. According to our discussion about Proposition 3.2, these residual connections enable the model to preserve the information of initial node features instead of exclusively smoothing node features.

For the computational efficiency, we mainly study the variations in the memory usage and the runtime as the number of model layers increases. From the memory side, according to Figure 3, our model requires less memory than all baseline models across different datasets, regardless of the number of layers used. In terms of the runtime, results in Figure 4 illustrate that our method is always within the

²Notably, we did not study the impact of the number of layers on SheafHyperGNN due to a lack of open-source code at the time of submission. For HGNN, HCHA, UniGNN, AllDeepSets, and AllSetTransformer, we use the code provided in Chien et al. (2022). For ED-HNN and PhenomNN, we use the code provided in Wang et al. (2023a) and Wang et al. (2023b) respectively.

Table 4: Ablation study on the GNN architecture and the weighted clique expansion used in WCE-GNN. The best result on each dataset is highlighted in **bold font**. CE denotes the unweighted clique expansion, and WCE denotes the clique expansion with edge weights generated by Eq. (5).

Models	Datasets			
	Cora-CA	DBLP-CA	Congress	Walmart
GAT+CE	81.83 ± 1.65	90.73 ± 0.35	86.30 ± 1.67	66.16 ± 0.70
GAT+WCE	81.83 ± 1.65	90.73 ± 0.35	86.30 ± 1.67	66.16 ± 0.70
SGC+CE	82.69 ± 1.55	90.14 ± 0.35	86.54 ± 1.83	65.86 ± 0.40
SGC+WCE	82.69 ± 1.55	90.15 ± 0.34	86.74 ± 1.81	65.95 ± 0.21
GCN+CE	80.86 ± 1.58	89.89 ± 0.38	84.72 ± 2.65	62.17 ± 0.60
GCN+WCE	80.90 ± 1.50	89.91 ± 0.42	85.47 ± 2.24	62.27 ± 0.56
GCNII+CE	84.99 ± 1.26	91.94 ± 0.22	89.02 ± 1.43	66.95 ± 0.50
GCNII+WCE	86.25 ± 1.25	92.16 ± 0.29	95.16 ± 1.03	68.92 ± 0.38

top three fastest models across all four different datasets, independent of the number of model layers. The results in Figures 3 and 4 empirically support our analysis at the end of Section 4 and exhibit that our model is remarkably efficient compared with existing HyperGNNs. This characteristic positions WCE-GNN as a promising choice for applications with limited computational resources.

Ablation study. In this part, we empirically study the efficiency of the GNN architecture and the edge weights in the weighted clique expansion utilised in our WCE-GNN. For the GNN architecture, we compare the GCNII, which is the architecture employed in our model, with three different GNN architectures: GAT (Veličković et al., 2018), SGC (Wu et al., 2019), and GCN (Kipf & Welling, 2017). The key distinction between GCNII and these architectures is that GCNII uniquely incorporates residual connections. Regarding the edge weights in weighted clique expansion, we contrast the clique expansion using weights calculated through our strategy with the unweighted clique expansion as introduced in Section 2.1. Based on the results summarised in Table 4, we observe that: 1) Regardless of the edge weights in the clique expansion, GCNII always achieves the best result, confirming that the usage of residual connections plays a crucial role in helping models produce

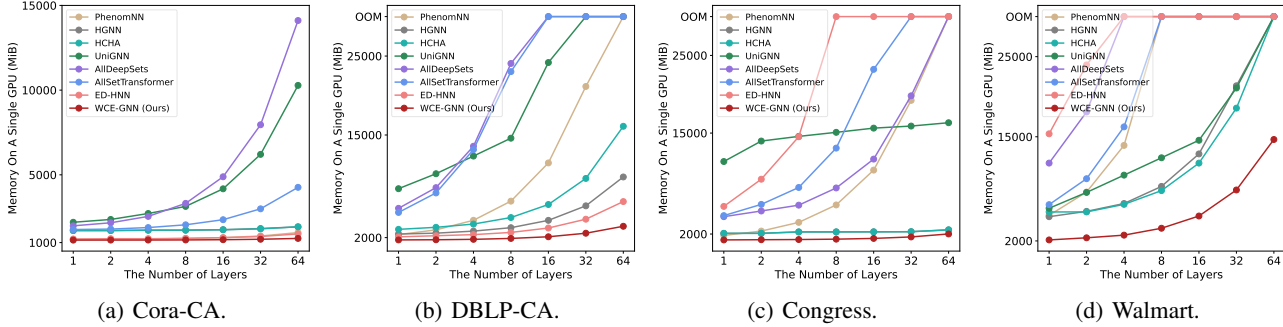


Figure 3: The impact of the number of model layers on the memory efficiency. Here, OOM indicates that the model encountered an Out Of Memory (OOM) issue during the experiment.

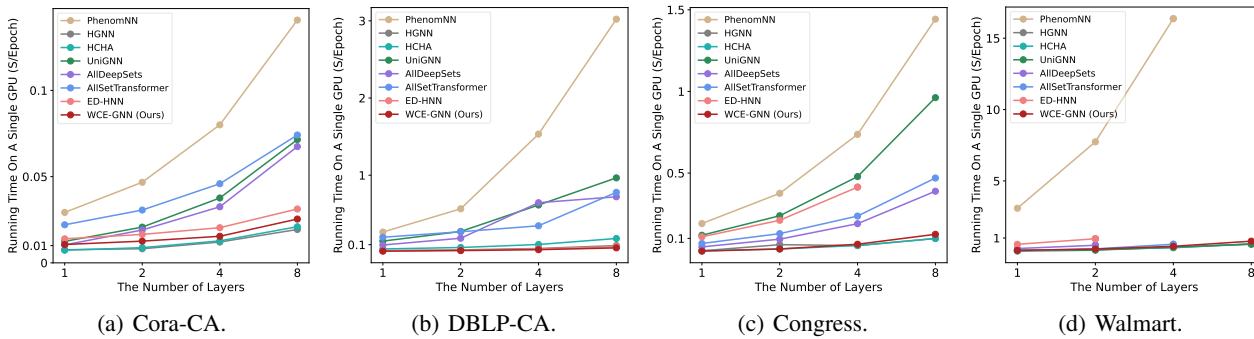


Figure 4: The impact of the number of model layers on the average runtime. We quantify the runtime by second per epoch and compute the average over 100 epochs where an epoch includes both the training and validation processes. Notably, some models experience an out-of-memory (OOM) issue when the layer count reaches a certain threshold, and we only report available results for such models.

suitable node features for hypergraph node classification; and 2) The model with the clique expansion using the edge weights generated by our strategy consistently outperforms a model with unweighted clique expansion, indicating that such edge weights are informative for the models. Notably, GAT shows the same results regardless of the edge weights in the clique expansion, as it learns the weight for each edge instead of using the pre-defined edge weights.

7. Conclusion & Limitation

Conclusion. In this paper, we conduct a theoretical analysis of the connections between GNNs and HyperGNNs in the context of hypergraph node classification, alongside a key theoretical contribution demonstrating that most HyperGNNs can be effectively approximated using a GNN equipped with a weighted clique expansion. This leads to the development of WCE-GNN, a simple and efficient learning framework designed for classifying nodes on hypergraphs. Extensive empirical evaluations show that WCE-GNN not only surpasses existing state-of-the-art Hyper-

GNNs on numerous datasets but also demonstrates promising resilience to the oversmoothing problem while having superior runtime and memory efficiency.

Our theoretical and empirical findings reveal that when GNNs are fed solely with pairwise interactions derived from a hypergraph, they perform comparably to HyperGNNs. This observation raises two pivotal questions for the hypergraph machine learning community: 1) Is the node classification task overly simplistic, thus rendering higher-order interactions unnecessary? and 2) Are current HyperGNN designs insufficiently capable of effectively capitalizing on higher-order interactions?

Limitation and future work. The hypergraph machine learning primarily includes two tasks: hypergraph node classification and hyperlink prediction. This paper focuses only on exploring the relationships between GNNs and HyperGNNs within the context of hypergraph node classification. The investigation of these connections in the domain of hyperlink prediction is left for our future research.

Impact Statements

This paper presents work whose goal is to advance the field of Machine Learning. There are many potential societal consequences of our work, none which we feel must be specifically highlighted here.

References

- Agarwal, S., Branson, K., and Belongie, S. Higher order learning with graphs. In *Proceedings of the 23rd international conference on Machine learning*, pp. 17–24, 2006.
- Antelmi, A., Cordasco, G., Polato, M., Scarano, V., Spagnuolo, C., and Yang, D. A survey on hypergraph representation learning. *ACM Computing Surveys*, 56(1):1–38, 2023.
- Atwood, J. and Towsley, D. Diffusion-convolutional neural networks. *Advances in neural information processing systems*, 29, 2016.
- Bai, S., Zhang, F., and Torr, P. H. Hypergraph convolution and hypergraph attention. *Pattern Recognition*, 110: 107637, 2021.
- Bick, C., Gross, E., Harrington, H. A., and Schaub, M. T. What are higher-order networks? *SIAM Review*, 65(3): 686–731, 2023.
- Bodnar, C., Di Giovanni, F., Chamberlain, B., Liò, P., and Bronstein, M. Neural sheaf diffusion: A topological perspective on heterophily and oversmoothing in gnns. *Advances in Neural Information Processing Systems*, 35: 18527–18541, 2022.
- Bolla, M. Spectra, euclidean representations and clusterings of hypergraphs. *Discrete Mathematics*, 117(1-3):19–39, 1993.
- Bronstein, M. M., Bruna, J., Cohen, T., and Veličković, P. Geometric deep learning: Grids, groups, graphs, geodesics, and gauges. *arXiv preprint arXiv:2104.13478*, 2021.
- Chen, M., Wei, Z., Huang, Z., Ding, B., and Li, Y. Simple and deep graph convolutional networks. In *International conference on machine learning*, pp. 1725–1735. PMLR, 2020.
- Chen, S., Eldar, Y. C., and Zhao, L. Graph unrolling networks: Interpretable neural networks for graph signal denoising. *IEEE Transactions on Signal Processing*, 69: 3699–3713, 2021.
- Chien, E., Pan, C., Peng, J., and Milenkovic, O. You are allset: A multiset function framework for hypergraph neural networks. In *International Conference on Learning Representations*, 2022. URL https://openreview.net/forum?id=hpBTIv2uy_E.
- Dong, Y., Sawin, W., and Bengio, Y. Hnhn: Hypergraph networks with hyperedge neurons. *ICML Graph Representation Learning and Beyond Workshop*, 2020. URL <https://arxiv.org/abs/2006.12278>.
- Duta, I., Cassarà, G., Silvestri, F., and Liò, P. Sheaf hypergraph networks, 2023.
- Feng, Y., You, H., Zhang, Z., Ji, R., and Gao, Y. Hypergraph neural networks. In *Proceedings of the AAAI conference on artificial intelligence*, volume 33, pp. 3558–3565, 2019.
- Gibson, D., Kleinberg, J., and Raghavan, P. Clustering categorical data: An approach based on dynamical systems. *The VLDB Journal*, 8:222–236, 2000.
- Gilmer, J., Schoenholz, S. S., Riley, P. F., Vinyals, O., and Dahl, G. E. Neural message passing for quantum chemistry. In *International conference on machine learning*, pp. 1263–1272. PMLR, 2017.
- Grone, R. and Merris, R. The laplacian spectrum of a graph ii. *SIAM Journal on discrete mathematics*, 7(2):221–229, 1994.
- Han, Y., Zhou, B., Pei, J., and Jia, Y. Understanding importance of collaborations in co-authorship networks: A supportiveness analysis approach. In *Proceedings of the 2009 SIAM International Conference on Data Mining*, pp. 1112–1123. SIAM, 2009.
- Horn, R. A. and Johnson, C. R. *Matrix analysis*. Cambridge university press, 2012.
- Huang, J. and Yang, J. Unignn: a unified framework for graph and hypergraph neural networks. In *Proceedings of the Thirtieth International Joint Conference on Artificial Intelligence, IJCAI-21*, 2021.
- Jhun, B. Effective epidemic containment strategy in hypergraphs. *Physical Review Research*, 3(3):033282, 2021.
- Kipf, T. N. and Welling, M. Semi-supervised classification with graph convolutional networks. In *International Conference on Learning Representations*, 2017. URL <https://openreview.net/forum?id=SJU4ayYgl>.
- Li, Q., Han, Z., and Wu, X.-M. Deeper insights into graph convolutional networks for semi-supervised learning. In *Proceedings of the AAAI conference on artificial intelligence*, volume 32, 2018.

- McPherson, M., Smith-Lovin, L., and Cook, J. M. Birds of a feather: Homophily in social networks. *Annual review of sociology*, 27(1):415–444, 2001.
- Meyer, C. D. and Stewart, I. *Matrix analysis and applied linear algebra*. SIAM, 2023.
- Mohar, B., Alavi, Y., Chartrand, G., and Oellermann, O. The laplacian spectrum of graphs. *Graph theory, combinatorics, and applications*, 2(871-898):12, 1991.
- Rusch, T. K., Bronstein, M. M., and Mishra, S. A survey on oversmoothing in graph neural networks. *arXiv preprint arXiv:2303.10993*, 2023.
- Veličković, P., Cucurull, G., Casanova, A., Romero, A., Liò, P., and Bengio, Y. Graph attention networks. In *International Conference on Learning Representations*, 2018. URL <https://openreview.net/forum?id=rJXMpikCZ>.
- Wang, P., Yang, S., Liu, Y., Wang, Z., and Li, P. Equivariant hypergraph diffusion neural operators. In *The Eleventh International Conference on Learning Representations*, 2023a. URL <https://openreview.net/forum?id=RiTjKoscnNd>.
- Wang, X. and Zhang, M. How powerful are spectral graph neural networks. In *International Conference on Machine Learning*, pp. 23341–23362. PMLR, 2022.
- Wang, Y., Gan, Q., Qiu, X., Huang, X., and Wipf, D. From hypergraph energy functions to hypergraph neural networks. In Krause, A., Brunskill, E., Cho, K., Engelhardt, B., Sabato, S., and Scarlett, J. (eds.), *Proceedings of the 40th International Conference on Machine Learning*, volume 202 of *Proceedings of Machine Learning Research*, pp. 35605–35623. PMLR, 23–29 Jul 2023b.
- Wei, T., You, Y., Chen, T., Shen, Y., He, J., and Wang, Z. Augmentations in hypergraph contrastive learning: Fabricated and generative. *Advances in neural information processing systems*, 35:1909–1922, 2022.
- Wu, F., Souza, A., Zhang, T., Fifty, C., Yu, T., and Weinberger, K. Simplifying graph convolutional networks. In *International conference on machine learning*, pp. 6861–6871. PMLR, 2019.
- Wu, Z., Pan, S., Chen, F., Long, G., Zhang, C., and Philip, S. Y. A comprehensive survey on graph neural networks. *IEEE transactions on neural networks and learning systems*, 32(1):4–24, 2020.
- Xu, K., Hu, W., Leskovec, J., and Jegelka, S. How powerful are graph neural networks? In *International Conference on Learning Representations*, 2019. URL <https://openreview.net/forum?id=ryGs6iA5Km>.
- Yadati, N., Nimishakavi, M., Yadav, P., Nitin, V., Louis, A., and Talukdar, P. Hypergcn: A new method for training graph convolutional networks on hypergraphs. In Wallach, H., Larochelle, H., Beygelzimer, A., d Alché-Buc, F., Fox, E., and Garnett, R. (eds.), *Advances in Neural Information Processing Systems*, volume 32. Curran Associates, Inc., 2019. URL <https://proceedings.neurips.cc/paper/2019/file/1efa39bcaec6f3900149160693694536-Paper.pdf>.
- Yang, Y., Liu, T., Wang, Y., Zhou, J., Gan, Q., Wei, Z., Zhang, Z., Huang, Z., and Wipf, D. Graph neural networks inspired by classical iterative algorithms. In *International Conference on Machine Learning*, pp. 11773–11783. PMLR, 2021.
- Zhou, D., Huang, J., and Schölkopf, B. Beyond pairwise classification and clustering using hypergraphs. 2005a.
- Zhou, D., Huang, J., and Schölkopf, B. Learning from labeled and unlabeled data on a directed graph. In *Proceedings of the 22nd international conference on Machine learning*, pp. 1036–1043, 2005b.

A. Reproducibility Statement.

Our code and data are available at: <https://github.com/tbh-98/WCE-GNN>.

B. Forward propagation layers of HyperGNNs discussed in our paper.

In this section, we formulate the forward propagation layers defined in five representative HyperGNNs using the matrix multiplication representation. These models include UniGNN (Huang & Yang, 2021), AllDeepSets (Chien et al., 2022), AllSetTransformer (Chien et al., 2022), ED-HNN (Wang et al., 2023a), and PhenomNN (Wang et al., 2023b). The first three of these models employ the two-step message passing mechanism. In contrast, ED-HNN is grounded in the diffusion mechanism, while PhenomNN is an unrolling-based method. Moreover, UniGNN, ED-HNN, and PhenomNN are equipped with the initial residual connection; in contrast, AllDeepSets and AllSetTransformer are not equipped with it.

For UniGNN (Huang & Yang, 2021), we introduce its forward propagation based on UniGCNII, which is the most powerful model based on this learning framework. Specifically, the l -th forward propagation layer of UniGNN (Huang & Yang, 2021) can be formulated as:

$$\begin{aligned} \mathbf{X}_{\mathcal{E}}^{(l)} &= \tilde{\mathbf{D}}_{\mathcal{H}^{\mathcal{E}}}^{-1/2} \mathbf{D}_{\mathcal{H}^{\mathcal{E}}}^{-1} \mathbf{H}^{\top} \mathbf{X}_{\mathcal{V}}^{(l-1)}, \\ \mathbf{X}_{\mathcal{V}}^{(l)} &= \sigma \left(\left((1-\gamma_U) \mathbf{D}_{\mathcal{H}^{\mathcal{V}}}^{-1/2} \mathbf{H} \mathbf{X}_{\mathcal{E}}^{(l)} + \gamma_U \mathbf{X}_{\mathcal{V}}^{(0)} \right) \Theta^{(l)} \right), \end{aligned} \quad (9)$$

where $\gamma_U \in \mathbb{R}$ is a hyperparameter, and $\tilde{\mathbf{D}}_{\mathcal{H}^{\mathcal{E}}} \in \mathbb{R}_+^{m \times m}$ is a diagonal matrix in which $\tilde{\mathbf{D}}_{\mathcal{H}^{\mathcal{E}}} = \frac{\sum_{i=1}^n \mathbf{H}_{ij} \mathbf{D}_{\mathcal{H}^{\mathcal{V}}}}{\mathbf{D}_{\mathcal{H}^{\mathcal{E}}}}$.

The l -th forward propagation layer of AllDeepSets (Chien et al., 2022) can be formulated as:

$$\begin{aligned} \mathbf{X}_{\mathcal{E}}^{(l)} &= \text{MLP}(\mathbf{D}_{\mathcal{H}^{\mathcal{E}}}^{-1} \mathbf{H}^{\top} \text{MLP}(\mathbf{X}_{\mathcal{V}}^{(l-1)})), \\ \mathbf{X}_{\mathcal{V}}^{(l)} &= \text{MLP}(\mathbf{D}_{\mathcal{H}^{\mathcal{V}}}^{-1} \mathbf{H} \text{MLP}(\mathbf{X}_{\mathcal{E}}^{(l)})), \end{aligned} \quad (10)$$

where $\text{MLP}(\cdot)$ denotes a multi-layer perceptron.

Without bias terms and normalisations, the l -th forward propagation layer of AllSetTransformer (Chien et al., 2022) can be formulated as:

$$\begin{aligned} \mathbf{X}_{\mathcal{E}}^{(l)} &= \text{MLP} \left(\bigoplus_{i \in \{1, \dots, h\}} \mathbf{H}^{\top} \text{D} \left(\sigma(\omega^{i^{\top}} \text{MLP}(\mathbf{X}_{\mathcal{V}}^{(l-1)^{\top}})) \right) \text{MLP}(\mathbf{X}_{\mathcal{V}}^{(l-1)}) \right) + \bigoplus_{i \in \{1, \dots, h\}} \mathbf{H}^{\top} \text{D} \left(\sigma(\omega^{i^{\top}} \text{MLP}(\mathbf{X}_{\mathcal{V}}^{(l-1)^{\top}})) \right) \text{MLP}(\mathbf{X}_{\mathcal{V}}^{(l-1)}), \\ \mathbf{X}_{\mathcal{V}}^{(l)} &= \text{MLP} \left(\bigoplus_{i \in \{1, \dots, h\}} \mathbf{H} \text{D} \left(\sigma(\omega^{i^{\top}} \text{MLP}(\mathbf{X}_{\mathcal{E}}^{(l)^{\top}})) \right) \text{MLP}(\mathbf{X}_{\mathcal{E}}^{(l)}) \right) + \bigoplus_{i \in \{1, \dots, h\}} \mathbf{H} \text{D} \left(\sigma(\omega^{i^{\top}} \text{MLP}(\mathbf{X}_{\mathcal{E}}^{(l)^{\top}})) \right) \text{MLP}(\mathbf{X}_{\mathcal{E}}^{(l)}), \end{aligned} \quad (11)$$

where $\text{MLP}(\cdot)$ denotes a multi-layer perceptron, $\text{D}(\cdot)$ is a function that transforms a given vector into a diagonal matrix, $\omega \in \mathbb{R}^d$ denotes some learnable parameters, and h is the number of attention heads. For simplicity, we set the number of attention heads as 1 in the following sections.

The l -th forward propagation layer of ED-HNN (Wang et al., 2023a) can be formulated as:

$$\begin{aligned} \mathbf{X}_{\mathcal{E}}^{(l)} &= \text{MLP} \left(\mathbf{D}_{\mathcal{H}^{\mathcal{E}}}^{-1} \mathbf{H}^{\top} \text{MLP}(\mathbf{X}_{\mathcal{V}}^{(l-1)}) \right), \\ \mathbf{X}_{\mathcal{V}}^{(l)} &= \text{MLP} \left((1-\gamma_E) \text{MLP}(\mathbf{D}_{\mathcal{H}^{\mathcal{V}}}^{-1} \mathbf{H} \mathbf{X}_{\mathcal{E}}^{(l)}) + \gamma_E \mathbf{X}_{\mathcal{V}}^{(0)} \right), \end{aligned} \quad (12)$$

where $\gamma_E \in (0, 1)$ is a hyperparameter, and $\text{MLP}(\cdot)$ denotes a multi-layer perceptron.

The l -th forward propagation layer of PhenomNN (Wang et al., 2023b) can be formulated as:

$$\begin{aligned} \mathbf{X}_{\mathcal{V}}^{(l)} &= \sigma \left((1-\gamma_2) \mathbf{X}_{\mathcal{V}}^{(l-1)} + \gamma_2 (\gamma_0 \mathbf{D}_C + \gamma_1 \mathbf{D}_{\mathcal{H}^{\mathcal{V}}} + \mathbf{I}_n)^{-1} \left[\mathbf{X}_{\mathcal{V}}^{(0)} + \gamma_0 (\mathbf{W}_C \mathbf{X}_{\mathcal{V}}^{(l-1)} (\Theta_0^{(l)} + \Theta_0^{(l)\top}) - \mathbf{D}_C \mathbf{X}_{\mathcal{V}}^{(l-1)} \Theta_0^{(l)} \Theta_0^{(l)\top}) \right. \right. \\ &\quad \left. \left. + \gamma_1 (\mathbf{D}_{\mathcal{H}^{\mathcal{V}}} - \mathbf{H} \mathbf{D}_{\mathcal{H}^{\mathcal{E}}}^{-1} \mathbf{H}^{\top}) \mathbf{X}_{\mathcal{V}}^{(l-1)} + \mathbf{H} \mathbf{D}_{\mathcal{H}^{\mathcal{E}}}^{-1} \mathbf{H}^{\top} \mathbf{X}_{\mathcal{V}}^{(l-1)} (\Theta_1^{(l)} + \Theta_1^{(l)\top}) - \mathbf{D}_{\mathcal{H}^{\mathcal{V}}} \mathbf{X}_{\mathcal{V}}^{(l-1)} \Theta_1^{(l)} \Theta_1^{(l)\top} \right] \right), \end{aligned} \quad (13)$$

where $\gamma_0, \gamma_1, \gamma_2 \in \mathbb{R}_+$ are three hyperparameters, $\mathbf{W}_C \in \mathbb{R}_{\geq 0}^{n \times n}$ is the adjacency matrix for an unweighted clique expansion

\mathcal{G}_C , and $\mathbf{D}_C \in \mathbb{R}_{\geq 0}^{n \times n}$ is the diagonal node degree matrix for \mathcal{G}_C .

C. Forward propagation layers of GNNs discussed in our paper.

For simplicity, and without loss of generality, we reformulate the forward propagation layer in Eq. (2) as follows:

$$\mathbf{X}_V^{(l)} = \sigma \left(\left((1 - \beta) \mathbf{W} \mathbf{X}_V^{(l-1)} + \beta \mathbf{X}_V^{(0)} \right) \hat{\Theta}^{(l)} \right), \quad (14)$$

where $\beta \in (0, 1)$.

Notably, in the following proofs, we use Eq. (14) to represent the forward propagation layer of the GNN.

D. Proof of Proposition 3.1.

Proof. We first prove that without non-linear activation, HyperGNNs operating on \mathcal{H} and GNNs operating on \mathcal{G} can be reformulated as a special case of the following formula:

$$\mathbf{x}_{v_i}^{(l)} = f_0(\mathbf{x}_{v_i}^{(l-1)}) + \rho f_1(\mathbf{x}_{v_i}^{(0)}) + \sum_{v_j \in \mathcal{N}_{\mathcal{G}_{v_i}}} f_2(\mathbf{x}_{v_j}^{(l-1)}), \quad (15)$$

For the feature update of v_i , without non-linear activation, UniGNN (Huang & Yang, 2021) formulated as Eq. (9) can be reformulated as:

$$\mathbf{x}_{v_i}^{(l)} = (1 - \gamma_U) \underbrace{\sum_{k=1}^m \frac{\mathbf{H}_{ik}}{\mathbf{D}_{\mathcal{H}_{kk}^\varepsilon} \mathbf{D}_{\mathcal{H}_{ii}^\nu} \tilde{\mathbf{D}}_{\mathcal{H}_{kk}^\varepsilon}^{1/2}} \mathbf{x}_{v_i}^{(l-1)} \Theta^{(l)}}_{f_0(\mathbf{x}_{v_i}^{(l-1)})} + \underbrace{\gamma_U \mathbf{x}_{v_i}^{(0)} \Theta^{(l)}}_{\rho f_1(\mathbf{x}_{v_i}^{(0)})} + \sum_{v_j \in \mathcal{N}_{\mathcal{G}_{v_i}}} \underbrace{\sum_{k=1}^m (1 - \gamma_U) \frac{\mathbf{H}_{ik} \mathbf{H}_{jk}}{\mathbf{D}_{\mathcal{H}_{kk}^\varepsilon} \mathbf{D}_{\mathcal{H}_{ii}^\nu} \tilde{\mathbf{D}}_{\mathcal{H}_{kk}^\varepsilon}^{1/2}} \mathbf{x}_{v_j}^{(l-1)} \Theta^{(l)}}_{f_2(\mathbf{x}_{v_j}^{(l-1)})}.$$

This formula is a special case of Eq. (15).

For the feature update of v_i , without non-linear activation, AllDeepSets (Chien et al., 2022) formulated as Eq. (10) can be reformulated as:

$$\mathbf{x}_{v_i}^{(l)} = \underbrace{\sum_{k=1}^m \frac{\mathbf{H}_{ik}}{\mathbf{D}_{\mathcal{H}_{kk}^\varepsilon} \mathbf{D}_{\mathcal{H}_{ii}^\nu}} \mathbf{x}_{v_i}^{(l-1)} \Theta^{(l)}}_{f_0(\mathbf{x}_{v_i}^{(l-1)})} + \sum_{v_j \in \mathcal{N}_{\mathcal{G}_{v_i}}} \underbrace{\sum_{k=1}^m \frac{\mathbf{H}_{ik} \mathbf{H}_{jk}}{\mathbf{D}_{\mathcal{H}_{kk}^\varepsilon} \mathbf{D}_{\mathcal{H}_{ii}^\nu}} \mathbf{x}_{v_j}^{(l-1)} \Theta^{(l)}}_{f_2(\mathbf{x}_{v_j}^{(l-1)})}.$$

This formula is a special case of Eq. (15).

For the feature update of v_i , without non-linear activation, AllSetTransformer (Chien et al., 2022) formulated as Eq. (11) can be reformulated as:

$$\mathbf{x}_{v_i}^{(l)} = \underbrace{\sum_{k=1}^m \mathbf{D}'_{\mathcal{H}_{ii}^\nu} \mathbf{D}'_{\mathcal{H}_{kk}^\varepsilon} \mathbf{H}_{ik} \mathbf{x}_{v_i}^{(l-1)} \Theta_0^{(l)}}_{f_0(\mathbf{x}_{v_i}^{(l-1)})} + \sum_{v_j \in \mathcal{N}_{\mathcal{G}_{v_i}}} \underbrace{\sum_{k=1}^m \mathbf{D}'_{\mathcal{H}_{jj}^\nu} \mathbf{D}'_{\mathcal{H}_{kk}^\varepsilon} \mathbf{H}_{ik} \mathbf{H}_{jk} \mathbf{x}_{v_j}^{(l-1)} \Theta_0^{(l)}}_{f_2(\mathbf{x}_{v_j}^{(l-1)})},$$

where $\mathbf{D}'_{\mathcal{H}^\nu} = \mathbf{D}(\omega \Theta_1^{(l)} \mathbf{X}_V^{(l-1)\top})$, and $\mathbf{D}'_{\mathcal{H}^\varepsilon} = \mathbf{D}(\omega \Theta_2^{(l)} \mathbf{X}_\mathcal{E}^{(l-1)\top})$. This formula is a special case of Eq. (15).

For the feature update of v_i , without non-linear activation, ED-HNN (Wang et al., 2023a) formulated as Eq. (12) can be reformulated as:

$$\mathbf{x}_{v_i}^{(l)} = (1 - \gamma_E) \underbrace{\sum_{k=1}^m \frac{\mathbf{H}_{ik}}{\mathbf{D}_{\mathcal{H}_{kk}^\varepsilon} \mathbf{D}_{\mathcal{H}_{ii}^\nu}} \mathbf{x}_{v_i}^{(l-1)} \Theta^{(l)}}_{f_0(\mathbf{x}_{v_i}^{(l-1)})} + \underbrace{\gamma_E \mathbf{x}_{v_i}^{(0)} \Theta^{(l)}}_{\rho f_1(\mathbf{x}_{v_i}^{(0)})} + \sum_{v_j \in \mathcal{N}_{\mathcal{G}_{v_i}}} \underbrace{(1 - \gamma_E) \sum_{k=1}^m \frac{\mathbf{H}_{ik} \mathbf{H}_{jk}}{\mathbf{D}_{\mathcal{H}_{kk}^\varepsilon} \mathbf{D}_{\mathcal{H}_{ii}^\nu}} \mathbf{x}_{v_j}^{(l-1)} \Theta^{(l)}}_{f_2(\mathbf{x}_{v_j}^{(l-1)})},$$

This formula is a special case of Eq. (15).

For the feature update of v_i , without non-linear activation, PhenomNN (Wang et al., 2023b) formulated as Eq. (13) can be

reformulated as:

$$\begin{aligned}
 \mathbf{x}_{v_i}^{(l)} &= (1-\gamma_2)\mathbf{x}_{v_i}^{(l-1)} - \underbrace{\frac{\gamma_0\gamma_2}{\gamma_0\mathbf{D}_{C_{ii}}+\gamma_1\mathbf{D}_{\mathcal{H}_{ii}^\gamma}+1}\mathbf{D}_{C_{ii}}\mathbf{x}_{v_i}^{(l-1)}\Theta_0\Theta_0^T - \frac{\gamma_1\gamma_2}{\gamma_0\mathbf{D}_{C_{ii}}+\gamma_1\mathbf{D}_{\mathcal{H}_{ii}^\gamma}+1}\mathbf{D}_{\mathcal{H}_{ii}^\gamma}\mathbf{x}_{v_i}^{(l-1)}(\Theta_1\Theta_1^T-\mathbf{I})}_{f_0(\mathbf{x}_{v_i}^{(l-1)})} \\
 &+ \underbrace{\frac{\gamma_2}{\gamma_0\mathbf{D}_{C_{ii}}+\gamma_1\mathbf{D}_{\mathcal{H}_{ii}^\gamma}+1}\mathbf{x}_{v_i}^{(0)}}_{\rho f_1(\mathbf{x}_{v_i}^{(0)})} \\
 &+ \underbrace{\sum_{v_j \in \mathcal{N}_{\mathcal{G}_{v_i}}} \left(\frac{\gamma_0\gamma_2}{\gamma_0\mathbf{D}_{C_{ii}}+\gamma_1\mathbf{D}_{\mathcal{H}_{ii}^\gamma}+1}\mathbf{W}_{C_{ij}}\mathbf{x}_{v_j}^{(l)}(\Theta_0^\top+\Theta_0) + \frac{\gamma_1\gamma_2}{\gamma_0\mathbf{D}_{C_{ii}}+\gamma_1\mathbf{D}_{\mathcal{H}_{ii}^\gamma}+1}\sum_{k=1}^m \frac{\mathbf{H}_{ik}\mathbf{H}_{jk}}{\mathbf{D}_{\mathcal{H}_{kk}^\varepsilon}}\mathbf{x}_{v_j}^{(l)}(\Theta_1^\top+\Theta_1-\mathbf{I}) \right)}_{f_2(\mathbf{x}_{v_j}^{(l-1)})}.
 \end{aligned}$$

This formula is a special case of Eq. (15).

For the feature update of v_i , without non-linear activation, the GNN formulated as Eq. (14) can be reformulated as:

$$\mathbf{x}_{v_i}^{(l)} = \underbrace{(1-\beta)\mathbf{W}_{N_{ii}}\mathbf{x}_{v_i}^{(l-1)}\hat{\Theta}^{(l)}}_{f_0(\mathbf{x}_{v_i}^{(l-1)})} + \underbrace{\beta\mathbf{x}_{v_i}^{(0)}\hat{\Theta}^{(l)}}_{\rho f_1(\mathbf{x}_{v_i}^{(0)})} + \sum_{v_j \in \mathcal{N}_{\mathcal{G}_{v_i}}} \underbrace{(1-\beta)\mathbf{W}_{N_{ij}}\mathbf{x}_{v_j}^{(l-1)}\hat{\Theta}^{(l)}}_{f_2(\mathbf{x}_{v_j}^{(l-1)})},$$

where $\mathbf{W}_N = (\mathbf{D} + \mathbf{I}_n)^{-1/2}(\mathbf{W} + \mathbf{I}_n)(\mathbf{D} + \mathbf{I}_n)^{-1/2}$. This is a special case of Eq. (15). Notably, when $\beta = 0$, this formula represents a GNN without the initial residual connection.

Based on the discussion above, when a HyperGNN/GNN incorporates the initial residual connection, $\mathcal{X}_{\mathcal{H}_{v_i}^l}^I = \mathcal{X}_{\mathcal{G}_{v_i}^l}^I = \{\mathbf{x}_{v_i}^{(l-1)}, \mathbf{x}_{v_i}^{(0)}, \oplus_{v_j \in \mathcal{N}_{\mathcal{G}_{v_i}}} \mathbf{x}_{v_j}^{(l-1)}\}$. In contrast, when a HyperGNN/GNN is implemented without the initial residual connection, $\mathcal{X}_{\mathcal{H}_{v_i}^l}^I = \mathcal{X}_{\mathcal{G}_{v_i}^l}^I = \{\mathbf{x}_{v_i}^{(l-1)}, \oplus_{v_j \in \mathcal{N}_{\mathcal{G}_{v_i}}} \mathbf{x}_{v_j}^{(l-1)}\}$. \square

E. Proof of Proposition 3.2.

We restate Proposition 3.2 as follows:

Proposition E.1. Let $\mathcal{H} = \{\mathcal{V}, \mathcal{E}, \mathbf{H}\}$ be a hypergraph, $\mathbf{D} \in \mathbb{R}^{n \times n}$ be the diagonal node degree matrix of \mathcal{G} , $\mathbf{X}_{\mathcal{V}}^{(0)} \in \mathbb{R}^{n \times d}$ be the initial node features, $\mathbf{X} \in \mathbb{R}^{n \times d}$, and $\mathbf{X}_{\mathcal{V}}^{(L)}$ denote the output of an L -layer HyperGNN/GNN. With non-linear activation removed, learnable parameters fixed and $L \rightarrow +\infty$, there exists a weighted clique expansion $\mathcal{G} = \{\mathcal{V}, \mathbf{W}\}$ of \mathcal{H} to make an L -layer HyperGNN/GNN operating on \mathcal{H}/\mathcal{G} have:

$$\lim_{L \rightarrow \infty} \mathbf{X}_{\mathcal{V}}^{(L)} = \arg \min_{\mathbf{X}} \text{tr}(\mathbf{X}^\top \mathbf{L} \mathbf{X}) + \rho \text{tr}[(\mathbf{X} - \mathbf{S} \mathbf{X}_{\mathcal{V}}^{(0)})^\top \mathbf{P}(\mathbf{X} - \mathbf{S} \mathbf{X}_{\mathcal{V}}^{(0)})], \quad (16)$$

where $\mathbf{L} \in \mathbb{R}^{n \times n}$ is the graph Laplacian of \mathcal{G} with $\mathbf{L} = \mathbf{D} - \mathbf{W}$, $\rho \in \mathbb{R}_{\geq 0}$ is a hyperparameter, $\mathbf{S} \in \mathbb{R}^{n \times n}$ is a diagonal matrix with \mathbf{S}_{ii} as the scalar of $\mathbf{x}_{v_i}^{(0)}$, and $\mathbf{P} \in \mathbb{R}_+^{n \times n}$ is a diagonal matrix with hyperparameter \mathbf{P}_{ii} that controls the importance of the initial features of v_i .

Before proving Proposition E.1, we first prove the following Lemmas.

Lemma E.1. When $\rho > 0$, the optimal solution \mathbf{X}^* for the optimisation formulated in the right-hand side of Eq. (16) is:

$$\mathbf{X}^* = \left(\mathbf{I}_n - (\mathbf{D} + \rho \mathbf{P})^{-1} \mathbf{W} \right)^{-1} (\mathbf{D} + \rho \mathbf{P})^{-1} \rho \mathbf{P} \mathbf{S} \mathbf{X}_{\mathcal{V}}^{(0)}. \quad (17)$$

Proof. Let $f(\mathbf{X}) = \text{tr}(\mathbf{X}^\top \mathbf{L} \mathbf{X}) + \rho \text{tr}[(\mathbf{X} - \mathbf{S} \mathbf{X}_{\mathcal{V}}^{(0)})^\top \mathbf{P}(\mathbf{X} - \mathbf{S} \mathbf{X}_{\mathcal{V}}^{(0)})]$, take the partial derivative of f with the respective of \mathbf{X} , we have:

$$\frac{\partial f}{\partial \mathbf{X}} = 2\mathbf{L}\mathbf{X} + 2\rho\mathbf{P}(\mathbf{X} - \mathbf{S}\mathbf{X}_{\mathcal{V}}^{(0)}).$$

By setting $\frac{\partial f}{\partial \mathbf{X}} = 0$, we have:

$$\mathbf{X}^* = (\mathbf{L} + \rho\mathbf{P})^{-1} \rho \mathbf{P} \mathbf{S} \mathbf{X}_{\mathcal{V}}^{(0)} = \left(\mathbf{I}_n - (\mathbf{D} + \rho\mathbf{P})^{-1} \mathbf{W} \right)^{-1} (\mathbf{D} + \rho\mathbf{P})^{-1} \rho \mathbf{P} \mathbf{S} \mathbf{X}_{\mathcal{V}}^{(0)},$$

Since the second-order derivative of f with the respect of \mathbf{X} is:

$$\frac{\partial^2 f}{\partial^2 \mathbf{X}} = 2\mathbf{L} + 2\rho\mathbf{P}. \quad (18)$$

Given $\mathbf{L} \in \mathbb{R}^{n \times n}$ is a graph Laplacian matrix, which is positive semi-definite, and $\mathbf{P} \in \mathbb{R}_+^{n \times n}$ is a diagonal matrix, which is positive definite, we have the righthand side of Eq.(18) is a positive definite matrix for $\rho > 0$. Hence, for $\rho > 0$, \mathbf{X}^* in Eq. (17) is the global minimal point for f , namely the solution for the optimisation formulated in the right-hand side of Eq. (16). \square

Lemma E.2. *When $\rho = 0$, if there exist an \mathbf{X}^* to make the value of the objective function in Eq. (16) equal to zero, such an \mathbf{X}^* is a solution for the optimisation formulated in the right-hand side of Eq. (16).*

Proof. When $\rho = 0$, the objective function in Eq. (16) can be reformulated as:

$$f(\mathbf{X}) = \text{tr}(\mathbf{X}^\top \mathbf{L} \mathbf{X}) = \sum_{i,j} \mathbf{W}_{ij} \|\mathbf{x}_i - \mathbf{x}_j\|_2^2. \quad (19)$$

Since \mathbf{W}_{ij} is the edge weight between v_i and v_j on the clique expansion, it is larger than 0. Then, we have:

$$f(\mathbf{X}) \geq 0.$$

Therefore, when $\rho = 0$, an \mathbf{X}^* reducing the objective function in Eq. (16) to zero is a solution for the optimisation formulated in the right-hand side of Eq. (16). \square

Lemma E.3. *Let $\mathbf{D} \in \mathbb{R}_{\geq 0}^{n \times n}$ be a fixed diagonal matrix with real positive diagonal elements, $\rho \in \mathbb{R}_+$ be an arbitrary real positive number, and $\mathbf{P} \in \mathbb{R}_{\geq 0}^{n \times n}$ be an arbitrary diagonal matrix with real positive diagonal elements. $(\mathbf{D} + \rho\mathbf{P})^{-1}$ can represent an arbitrary diagonal matrix $\mathbf{M} \in \mathbb{R}_{\geq 0}^{n \times n}$ with $\frac{1}{\mathbf{D}_{ii}} > \mathbf{M}_{ii}$.*

Proof. We can have:

$$[(\mathbf{D} + \rho\mathbf{P})^{-1}]_{ii} = \frac{1}{\mathbf{D}_{ii} + \rho\mathbf{P}_{ii}} \quad (20)$$

Since $\rho, \mathbf{P}_{ii} \in \mathbb{R}_+$ are two arbitrary real positive numbers, we can reformulate Eq. (23) as:

$$[(\mathbf{D} + \rho\mathbf{P})^{-1}]_{ii} = \frac{1}{k+x} \quad (21)$$

where $k \in \mathbb{R}_+$ is a fixed real positive number, and $x \in \mathbb{R}_+$ is an arbitrary real positive number. As $f(x) = \frac{1}{k+x} \in (0, \frac{1}{k})$ for any $x \in (0, +\infty)$, we have $[(\mathbf{D} + \rho\mathbf{P})^{-1}]_{ii}$ in $(0, \frac{1}{\mathbf{D}_{ii}})$. \square

Lemma E.4. *Let $\mathbf{P} \in \mathbb{R}_{\geq 0}^{n \times n}$ be a fixed diagonal matrix with real positive diagonal elements, $\mathbf{D} \in \mathbb{R}_{\geq 0}^{n \times n}$ be a fixed diagonal matrix with real positive diagonal elements, $\rho \in \mathbb{R}_+$ be a fixed real positive number, and $\mathbf{S} \in \mathbb{R}_{\geq 0}^{n \times n}$ be an arbitrary diagonal matrix with real positive diagonal elements. $(\mathbf{D} + \rho\mathbf{P})^{-1} \rho\mathbf{P}\mathbf{S}$ can represent an arbitrary diagonal matrix $\mathbf{M} \in \mathbb{R}_{\geq 0}^{n \times n}$ with real positive diagonal elements.*

Proof. We can have:

$$[(\mathbf{D} + \rho\mathbf{P})^{-1} \rho\mathbf{P}\mathbf{S}]_{ii} = \frac{\rho\mathbf{P}_{ii}}{\mathbf{D}_{ii} + \rho\mathbf{P}_{ii}} \mathbf{S}_{ii} \quad (22)$$

Since $\mathbf{S}_{ii} \in \mathbb{R}_+$ is an arbitrary real positive number, we can reformulate Eq. (22) as:

$$[(\mathbf{D} + \rho\mathbf{P})^{-1} \rho\mathbf{P}\mathbf{S}]_{ii} = kx \quad (23)$$

where $k \in \mathbb{R}_+$ is a fixed real positive number, and $x \in \mathbb{R}_+$ is an arbitrary real positive number. As $f(x) = kx \in (0, +\infty)$ for any $x \in (0, +\infty)$, we have $[(\mathbf{D} + \rho\mathbf{P})^{-1} \rho\mathbf{P}\mathbf{S}]_{ii}$ can be an arbitrary real positive number. \square

Lemma E.5. *Let $\mathbf{H} \in \{0, 1\}^{n \times m}$ be an incidence matrix of a hypergraph, $\mathbf{D}_{\mathcal{H}^\vee} \in \mathbb{R}^{n \times n}$ be a diagonal matrix with node degrees, and $\mathbf{D}_{\mathcal{H}^\varepsilon} \in \mathbb{R}^{m \times m}$ be a diagonal matrix with hyperedge degrees. We have $\sum_{j=1}^n \sum_{k=1}^m \frac{\mathbf{H}_{ik}\mathbf{H}_{jk}}{\mathbf{D}_{\mathcal{H}^\varepsilon_{kk}}} = \mathbf{D}_{\mathcal{H}^\vee_{ii}}$.*

Proof. We have:

$$\sum_{j=1}^n \sum_{k=1}^m \frac{\mathbf{H}_{ik}\mathbf{H}_{jk}}{\mathbf{D}_{\mathcal{H}^\varepsilon_{kk}}} = \sum_{e_k \in \mathcal{E}_{v_i}} \sum_{v_j \in e_k} \frac{\mathbf{H}_{jk}}{\mathbf{D}_{\mathcal{H}^\varepsilon_{kk}}} = \mathbf{D}_{\mathcal{H}^\vee_{ii}},$$

where \mathcal{E}_{v_i} is a set containing hyperedges with v_i . \square

Lemma E.6. Let $\mathbf{H} \in \{0, 1\}^{n \times m}$ be an incidence matrix of a hypergraph, $\mathbf{D}_{\mathcal{H}^\nu} \in \mathbb{R}^{n \times n}$ is a diagonal matrix with node degrees, $\mathbf{D}_{\mathcal{H}^\varepsilon} \in \mathbb{R}^{m \times m}$ is a diagonal matrix with hyperedge degrees, $\tilde{\mathbf{D}}_{\mathcal{H}^\varepsilon} \in \mathbb{R}^{m \times m}$ is a diagonal matrix with $\tilde{\mathbf{D}}_{\mathcal{H}^\varepsilon} = \frac{\sum_{i=1}^n \mathbf{H}_{ij} \mathbf{D}_{\mathcal{H}^\nu_{ii}}}{\mathbf{D}_{\mathcal{H}^\varepsilon_{jj}}}$ and $\mathbf{W}_U = \mathbf{H} \tilde{\mathbf{D}}_{\mathcal{H}^\varepsilon}^{-1/2} \mathbf{D}_{\mathcal{H}^\nu}^{-1} \mathbf{H}^\top$. We have: 1) \mathbf{W}_U is the adjacency matrix of a weighted clique expansion with eigendecomposition; 2) Let \mathbf{D}_U be the diagonal node degree matrix corresponding to \mathbf{W}_U , for $\gamma_U \in [1 - \frac{1}{\sqrt{m}}, 1)$, we have $\frac{1}{\mathbf{D}_{U_{ii}}} > \frac{1-\gamma_U}{\mathbf{D}_{\mathcal{H}^\nu_{ii}}^{1/2}}$; 3) $\mathbf{W}_{U'} = (1 - \gamma_U) \mathbf{D}_{\mathcal{H}^\nu}^{-1/2} \mathbf{W}_U$ is the adjacency matrix of a weighted clique expansion with eigendecomposition; and 4) For $\gamma_U \in [1 - \frac{1}{\sqrt{m}}, 1)$, we have the absolute values of eigenvalues of $\mathbf{W}_{U'}$ are less than 1 and $\det(\mathbf{W}_{U'}) < 1$.

Proof. We have:

$$\mathbf{W}_{U_{ij}} = \sum_{k=1}^m \frac{\mathbf{H}_{ik} \mathbf{H}_{jk}}{\mathbf{D}_{\mathcal{H}^\varepsilon_{kk}} \tilde{\mathbf{D}}_{\mathcal{H}^\varepsilon_{kk}}^{1/2}}.$$

Here $\mathbf{W}_{U_{ij}} > 0$ if and only if v_i and v_j are connected by a hyperedge on \mathcal{H} , otherwise $\mathbf{W}_{U_{ij}} = 0$. Therefore, \mathbf{W}_U is the adjacency matrix of a weighted clique expansion. Moreover, since \mathbf{W}_U is a real symmetric matrix, it has eigendecomposition.

Let \mathbf{D}_U be the diagonal node degree matrix corresponding to \mathbf{W}_U , based on Lemma E.5, we have:

$$\frac{\mathbf{D}_{U_{ii}}}{\mathbf{D}_{\mathcal{H}^\nu_{ii}}^{1/2}} = \sum_{j=1}^n \sum_{k=1}^m \frac{\mathbf{H}_{ik} \mathbf{H}_{jk}}{\mathbf{D}_{\mathcal{H}^\varepsilon_{kk}} \mathbf{D}_{\mathcal{H}^\nu_{ii}}^{1/2} \tilde{\mathbf{D}}_{\mathcal{H}^\varepsilon_{kk}}^{1/2}} < \sum_{j=1}^n \sum_{k=1}^m \frac{\mathbf{H}_{ik} \mathbf{H}_{jk}}{\mathbf{D}_{\mathcal{H}^\varepsilon_{kk}} \mathbf{D}_{\mathcal{H}^\nu_{ii}}^{1/2}} = \mathbf{D}_{\mathcal{H}^\nu_{ii}}^{1/2}.$$

Therefore, for $\gamma_U \in [1 - \frac{1}{\sqrt{m}}, 1)$, we have:

$$\frac{\mathbf{D}_{U_{ii}}}{\mathbf{D}_{\mathcal{H}^\nu_{ii}}^{1/2}} < \mathbf{D}_{\mathcal{H}^\nu_{ii}}^{1/2} \leq \sqrt{m} \leq \frac{1}{1 - \gamma_U} \Leftrightarrow \frac{1}{\mathbf{D}_{U_{ii}}} > \frac{1 - \gamma_U}{\mathbf{D}_{\mathcal{H}^\nu_{ii}}^{1/2}}. \quad (24)$$

$\mathbf{W}_{U'}$ is a row-normalised \mathbf{W}_U and is similar to $(1 - \gamma_U) \mathbf{D}_{\mathcal{H}^\nu}^{-1/4} \mathbf{W}_U \mathbf{D}_{\mathcal{H}^\nu}^{-1/4}$, which is a real symmetric matrix, so it is the adjacency matrix of a weighted clique expansion with eigendecomposition. Moreover, based on Eq. (24), the sum of each row of $\mathbf{W}_{U'}$ is less than 1 as:

$$(1 - \gamma_U) \sum_{j=1}^n \sum_{k=1}^m \frac{\mathbf{H}_{ik} \mathbf{H}_{jk}}{\mathbf{D}_{\mathcal{H}^\varepsilon_{kk}} \mathbf{D}_{\mathcal{H}^\nu_{ii}}^{1/2} \tilde{\mathbf{D}}_{\mathcal{H}^\varepsilon_{kk}}^{1/2}} < (1 - \gamma_U) \sum_{j=1}^n \sum_{k=1}^m \frac{\mathbf{H}_{ik} \mathbf{H}_{jk}}{\mathbf{D}_{\mathcal{H}^\varepsilon_{kk}} \mathbf{D}_{\mathcal{H}^\nu_{ii}}^{1/2}} \leq \frac{\mathbf{D}_{\mathcal{H}^\nu_{ii}}^{1/2}}{\sqrt{m}} \leq 1.$$

Since $\mathbf{W}_{U'}$ is a matrix with non-negative elements, according to the Gershgorin circle theorem (Horn & Johnson, 2012), we have the absolute values of eigenvalues of $\mathbf{W}_{U'}$ are less than 1 and $\det(\mathbf{W}_{U'}) < 1$. \square

Lemma E.7. Let $\mathbf{H} \in \{0, 1\}^{n \times m}$ be an incidence matrix of a hypergraph, $\mathbf{D}_{\mathcal{H}^\nu} \in \mathbb{R}^{n \times n}$ be a diagonal matrix with node degrees, and $\mathbf{D}_{\mathcal{H}^\varepsilon} \in \mathbb{R}^{m \times m}$ be a diagonal matrix with hyperedge degrees. We have: 1) $\mathbf{W}_S = \mathbf{H} \mathbf{D}_{\mathcal{H}^\varepsilon}^{-1} \mathbf{H}^\top$ is the adjacency matrix of a weighted clique expansion with eigendecomposition; 2) Let $\mathbf{D}_S \in \mathbb{R}^{n \times n}$ be a diagonal matrix contain the node degrees corresponding to \mathbf{W}_S , we have $\mathbf{D}_S = \mathbf{D}_{\mathcal{H}^\nu}$; and 3) $\mathbf{W}_{S'} = \mathbf{D}_{\mathcal{H}^\nu}^{-1} \mathbf{H} \mathbf{D}_{\mathcal{H}^\varepsilon}^{-1} \mathbf{H}^\top$ is the row-normalised adjacency matrix of a weighted clique expansion having an eigendecomposition with $\det(\mathbf{W}_{S'}) \leq 1$.

Proof. We have:

$$\mathbf{W}_{S_{ij}} = \sum_{k=1}^m \frac{\mathbf{H}_{ik} \mathbf{H}_{jk}}{\mathbf{D}_{\mathcal{H}^\varepsilon_{kk}}}.$$

Here $\mathbf{W}_{S_{ij}} > 0$ if and only if v_i and v_j are connected by a hyperedge on \mathcal{H} , otherwise $\mathbf{W}_{S_{ij}} = 0$. Therefore, \mathbf{W}_S is the adjacency matrix of a weighted clique expansion. Moreover, since \mathbf{W}_S is a real symmetric matrix, it has eigendecomposition. Let \mathbf{D}_S be the diagonal node degree matrix corresponding to \mathbf{W}_S , based on Lemma E.5, we have $\mathbf{D}_S = \mathbf{D}_{\mathcal{H}^\nu}$. Therefore $\mathbf{W}_{S'}$ is a row-normalised \mathbf{W}_S , which is normalised by \mathbf{D}_S , and it is similar to $\mathbf{D}_{\mathcal{H}^\nu}^{-1/2} \mathbf{H} \mathbf{D}_{\mathcal{H}^\varepsilon}^{-1} \mathbf{H}^\top \mathbf{D}_{\mathcal{H}^\nu}^{-1/2}$, which is a real symmetric matrix. As a result, $\mathbf{W}_{S'} \in \mathbb{R}_+^{n \times n}$ is the adjacency matrix of a weighted clique expansion having an eigendecomposition. Since the sum of each row of $\mathbf{W}_{S'}$ is 1, according to the Gershgorin circle theorem (Horn & Johnson, 2012), we have $\det(\mathbf{W}_{S'}) \leq 1$. \square

Lemma E.8. Let $\mathbf{H} \in \{0, 1\}^{n \times m}$ be an incidence matrix of a hypergraph, $\mathbf{D}'_{\mathcal{H}^\nu} \in \mathbb{R}^{n \times n}$ is a diagonal matrix, and $\mathbf{D}'_{\mathcal{H}^\varepsilon}$ is a diagonal matrix. We have: 1) $\mathbf{W}_T = \mathbf{H}\mathbf{D}'_{\mathcal{H}^\varepsilon}\mathbf{H}^\top\mathbf{D}'_{\mathcal{H}^\nu}$ is a weighted clique expansion with eigendecomposition; and 2) When the maximum value in $\mathbf{D}'_{\mathcal{H}^\nu}$ and $\mathbf{D}'_{\mathcal{H}^\varepsilon}$ within $(0, \frac{1}{\sqrt{mn}})$, the eigenvalues of \mathbf{W}_T are within $(-1, 1)$.

Proof. We have:

$$\mathbf{W}_{T_{ij}} = \sum_{k=1}^m \mathbf{D}'_{\mathcal{H}^\nu_{jj}} \mathbf{D}'_{\mathcal{H}^\varepsilon_{kk}} \mathbf{H}_{ik} \mathbf{H}_{jk}.$$

Here $\mathbf{W}_{T_{ij}} > 0$ if and only if v_i and v_j are connected by a hyperedge on \mathcal{H} , otherwise $\mathbf{W}_{T_{ij}} = 0$. Therefore, \mathbf{W}_T is the adjacency matrix of a weighted clique expansion. Moreover, since \mathbf{W}_T is similar to $\mathbf{D}'_{\mathcal{H}^\nu} \mathbf{H} \mathbf{D}'_{\mathcal{H}^\varepsilon} \mathbf{H}^\top \mathbf{D}'_{\mathcal{H}^\nu}$, which is a real symmetric matrix, it has eigendecomposition.

If the maximum value in $\mathbf{D}'_{\mathcal{H}^\nu}$ and $\mathbf{D}'_{\mathcal{H}^\varepsilon}$ within $(0, \frac{1}{\sqrt{mn}})$, we can formulate the sum of each row in \mathbf{W}_T as:

$$\sum_{j=1}^n \sum_{k=1}^m \mathbf{D}'_{\mathcal{H}^\nu_{jj}} \mathbf{D}'_{\mathcal{H}^\varepsilon_{kk}} \mathbf{H}_{ik} \mathbf{H}_{jk} \leq \sum_{j=1}^n \sum_{k=1}^m \mathbf{D}'_{\mathcal{H}^\nu_{jj}} \mathbf{D}'_{\mathcal{H}^\varepsilon_{kk}} \leq mn \mathbf{D}'_{\mathcal{H}^\nu_{max}} \mathbf{D}'_{\mathcal{H}^\varepsilon_{max}} < 1.$$

According to the Gershgorin circle theorem (Horn & Johnson, 2012), we have the eigenvalues of \mathbf{W}_T are within $(-1, 1)$. \square

Lemma E.9. Let $\mathbf{H} \in \{0, 1\}^{n \times m}$ be an incidence matrix of a hypergraph, $\mathbf{D}_{\mathcal{H}^\nu} \in \mathbb{R}^{n \times n}$ be a diagonal matrix with node degrees, $\mathbf{D}_{\mathcal{H}^\varepsilon} \in \mathbb{R}^{m \times m}$ be a diagonal matrix with hyperedge degrees, $\mathbf{W}_C \in \mathbb{R}_{\geq 0}^{n \times n}$ be the adjacency matrix for an unweighted clique expansion \mathcal{G}_C corresponding to \mathbf{H} , $\gamma_0, \gamma_1, \gamma_2 \in \mathbb{R}_+$ be three hyperparameters, $\mathbf{D}_C \in \mathbb{R}_{\geq 0}^{n \times n}$ be the diagonal node degree matrix for \mathcal{G}_C , and $\tilde{\mathbf{D}}^{-1} = \frac{1}{2}(\gamma_0 \mathbf{D}_C + \gamma_1 \mathbf{D}_{\mathcal{H}^\nu} + \mathbf{I}_n)^{-1}$. We have 1) $\mathbf{W}_P = \lambda_1 \mathbf{D}_{\mathcal{H}^\nu} + \mathbf{I}_n + 2\lambda_0 \mathbf{W}_C + \lambda_1 \mathbf{H} \mathbf{D}_{\mathcal{H}^\varepsilon}^{-1} \mathbf{H}^\top$ is the adjacency matrix of a weighted clique expansion with eigendecomposition; 2) Let \mathbf{D}_P be the diagonal node degree matrix corresponding to \mathbf{W}_P , we have $\frac{1}{\mathbf{D}_{P_{ii}}} > \tilde{\mathbf{D}}_{ii}^{-1}$; 3) The eigenvalues of $\tilde{\mathbf{D}}^{-1} \mathbf{W}_P$ are within $(-1, 1)$; and 4) $\det(\tilde{\mathbf{D}}^{-1} \mathbf{W}_P) < 1$.

Proof. We have:

$$\mathbf{W}_{P_{ij}} = 2\lambda_0 \tau\left(\sum_{k=1}^m \mathbf{H}_{ik} \mathbf{H}_{jk}\right) + \sum_{k=1}^m \frac{\lambda_1 \mathbf{H}_{ik} \mathbf{H}_{jk}}{\mathbf{D}_{\mathcal{H}^\varepsilon_{kk}}},$$

where $\tau(x) = 1$ if and only if $x > 0$, otherwise $\tau(x) = 0$. Here $\mathbf{W}_{P_{ij}} > 0$ if and only if v_i and v_j are connected by a hyperedge on \mathcal{H} , otherwise $\mathbf{W}_{P_{ij}} = 0$. Therefore, \mathbf{W}_P is the adjacency matrix of a weighted clique expansion. Moreover, since \mathbf{W}_P is a real symmetric matrix, it has eigendecomposition. Let \mathbf{D}_P be the diagonal node degree matrix corresponding to \mathbf{W}_P , based on Lemma E.5, we have:

$$\mathbf{D}_{P_{ii}} = 1 + \lambda_1 \mathbf{D}_{\mathcal{H}^\nu_{ii}} + \sum_{j=1}^n [2\lambda_0 \tau\left(\sum_{k=1}^m \mathbf{H}_{ik} \mathbf{H}_{jk}\right) + \sum_{k=1}^m \frac{\lambda_1 \mathbf{H}_{ik} \mathbf{H}_{jk}}{\mathbf{D}_{\mathcal{H}^\varepsilon_{kk}}}] = 1 + 2\lambda_0 \mathbf{D}_{C_{ii}} + 2\lambda_1 \mathbf{D}_{\mathcal{H}^\nu_{ii}}.$$

For $\tilde{\mathbf{D}}^{-1}$, we have:

$$\tilde{\mathbf{D}}_{ii}^{-1} = \frac{1}{2 + 2\lambda_0 \mathbf{D}_{C_{ii}} + 2\lambda_1 \mathbf{D}_{\mathcal{H}^\nu_{ii}}}.$$

Hence, we have $\frac{1}{\mathbf{D}_{P_{ii}}} > \tilde{\mathbf{D}}_{ii}^{-1}$, and the sum of each row of $\tilde{\mathbf{D}}^{-1} \mathbf{W}_P$ is less than 1. Since $\tilde{\mathbf{D}}^{-1} \mathbf{W}_P$ with non-negative elements, according to the Gershgorin circle theorem (Horn & Johnson, 2012), we have the eigenvalues of $\tilde{\mathbf{D}}^{-1} \mathbf{W}_P$ are within $(-1, 1)$ and $\det(\tilde{\mathbf{D}}^{-1} \mathbf{W}_P) < 1$. \square

With the Lemmas above, we present the proof of Proposition E.1 as follows.

Proof. For an L -layer UniGNN (Huang & Yang, 2021), devoid non-linear activation and by setting the learnable transformation matrix to the identity matrix, it can be reformulated as:

$$\mathbf{X}_\nu^{(L)} = \left((1 - \gamma_U)^L (\mathbf{D}_{\mathcal{H}^\nu}^{-1/2} \mathbf{H} \tilde{\mathbf{D}}_{\mathcal{H}^\varepsilon}^{-1/2} \mathbf{D}_{\mathcal{H}^\varepsilon}^{-1} \mathbf{H}^\top)^L + \gamma_U \sum_{l=0}^{L-1} (1 - \gamma_U)^l (\mathbf{D}_{\mathcal{H}^\nu}^{-1/2} \mathbf{H} \tilde{\mathbf{D}}_{\mathcal{H}^\varepsilon}^{-1/2} \mathbf{D}_{\mathcal{H}^\varepsilon}^{-1} \mathbf{H}^\top)^l \right) \mathbf{X}_\nu^{(0)}. \quad (25)$$

For simplicity, we further set $\gamma_U \in [1 - \frac{1}{\sqrt{m}}, 1)$. Then, based on Lemma E.6, when $L \rightarrow +\infty$, the left term tends to $\mathbf{0}$ and the right term becomes a convergent geometric series (Meyer & Stewart, 2023). Hence we have:

$$\mathbf{X}_\nu^{(+\infty)} = \gamma_U (\mathbf{I}_n - (1 - \gamma_U) \mathbf{D}_{\mathcal{H}^\nu}^{-1/2} \mathbf{W}_U)^{-1} \mathbf{X}_\nu^{(0)},$$

where $\mathbf{W}_U = \mathbf{H}\tilde{\mathbf{D}}_{\mathcal{H}^\varepsilon}^{-1/2}\mathbf{D}_{\mathcal{H}^\varepsilon}^{-1}\mathbf{H}^\top$. Based on Lemma E.3, E.4 and E.6, for $\gamma_U \in [1 - \frac{1}{\sqrt{m}}, 1)$, this formula is a special case of Eq. (17), when $\mathbf{W} = \mathbf{W}_U$, $(\mathbf{D} + \rho\mathbf{P})^{-1} = (1 - \gamma_U)\mathbf{D}_{\mathcal{H}^\nu}^{-1/2}$ and $(\mathbf{D} + \rho\mathbf{P})^{-1}\rho\mathbf{P}\mathbf{S} = \gamma_U\mathbf{I}_n$. Based on Lemma E.1, UniGNN can solve the optimisation formulated in the right-hand side of Eq. (16) with $\rho > 0$ and $\mathbf{W} = \mathbf{W}_U$.

For anyDeepSets (Chien et al., 2022) formulated as Eq. (10), devoid non-linear activation and by setting the learnable transformation matrix to the identity matrix, we have:

$$\mathbf{X}_\nu^{(L)} = \mathbf{W}_{S'}^L \mathbf{X}_\nu^{(0)}, \quad (26)$$

where $\mathbf{W}_S = \mathbf{H}\mathbf{D}_{\mathcal{H}^\varepsilon}^{-1}\mathbf{H}^\top$ and $\mathbf{W}_{S'} = \mathbf{D}_{\mathcal{H}^\nu}^{-1}\mathbf{W}_S$. Based on Lemma E.7, $\mathbf{W}_{S'}$ is a row-normalised graph adjacency matrix. Therefore, according to the Theorem 1 in Li et al. (2018), we have, when $L \rightarrow +\infty$, features of connected nodes in $\mathbf{X}_\nu^{(L)}$ defined in Eq. (26) being identical. As a result, based on Eq. (19) these features would make the objective function in Eq. (16) equal to zero for $\rho = 0$. Based on Lemma E.2, AllDeepSets can solve the optimisation formulated in the right-hand side of Eq. (16) with $\rho = 0$ and $\mathbf{W} = \mathbf{W}_S$.

For anySetTransformer (Chien et al., 2022) formulated as Eq. (11), devoid non-linear activation and by setting the learnable transformation matrix to the identity matrix, we have:

$$\mathbf{X}_\nu^{(L)} = \mathbf{W}_T^L \mathbf{X}_\nu^{(0)} \quad (27)$$

where $\mathbf{W}_T = (\mathbf{H}\mathbf{D}'_{\mathcal{H}^\varepsilon}\mathbf{H}^\top\mathbf{D}'_{\mathcal{H}^\nu})$, $\mathbf{D}'_{\mathcal{H}^\nu} = \mathbf{D}(\omega\mathbf{X}_\nu^{(l-1)\top})$, and $\mathbf{D}'_{\mathcal{H}^\varepsilon} = \mathbf{D}(\omega\mathbf{X}_\varepsilon^{(l-1)\top})$. We fix ω as a vector containing parameters that make the maximum value in $\mathbf{D}'_{\mathcal{H}^\nu}$ and $\mathbf{D}'_{\mathcal{H}^\varepsilon}$ within $(0, \frac{1}{\sqrt{mn}})$. Based on Lemma E.8 we have:

$$\mathbf{X}_\nu^{(+\infty)} = \mathbf{0}.$$

This makes the objective function in Eq. (16) equal to zero. Based on Lemma E.2 and E.8, AllSetTransformer can solve the optimisation formulated in the right-hand side of Eq. (16) with $\rho = 0$ and $\mathbf{W} = \mathbf{W}_T$.

For ED-HNN (Wang et al., 2023a) formulated as Eq. (12), devoid non-linear activation and by setting the learnable transformation matrix to the identity matrix, we have:

$$\mathbf{X}_\nu^{(L)} = \left((1 - \gamma_E)^L (\mathbf{D}_{\mathcal{H}^\nu}^{-1} \mathbf{H} \mathbf{D}_{\mathcal{H}^\varepsilon}^{-1} \mathbf{H}^\top)^L + \gamma_E \sum_{l=0}^{L-1} (1 - \gamma_E)^l (\mathbf{D}_{\mathcal{H}^\nu}^{-1} \mathbf{H} \mathbf{D}_{\mathcal{H}^\varepsilon}^{-1} \mathbf{H}^\top)^l \right) \mathbf{X}_\nu^{(0)}. \quad (28)$$

Based on Lemma E.7, for $\gamma_E \in (0, 1)$, when $L \rightarrow +\infty$, the left term tends to $\mathbf{0}$ and the right term becomes a convergent geometric series (Meyer & Stewart, 2023). Hence we have:

$$\mathbf{X}_\nu^{(+\infty)} = \gamma_E (\mathbf{I}_n - (1 - \gamma_E) \mathbf{D}_{\mathcal{H}^\nu}^{-1} \mathbf{W}_S)^{-1} \mathbf{X}_\nu^{(0)}.$$

where $\mathbf{W}_S = \mathbf{H}\mathbf{D}_{\mathcal{H}^\varepsilon}^{-1}\mathbf{H}^\top$. Based on Lemma E.3, E.4 and E.7, for $\gamma_E \in (0, 1)$, this formula is a special case of Eq. (17), when $\mathbf{W} = \mathbf{W}_S$, $(\mathbf{D} + \rho\mathbf{P})^{-1} = (1 - \gamma_E)\mathbf{D}_{\mathcal{H}^\nu}^{-1}$ and $(\mathbf{D} + \rho\mathbf{P})^{-1}\rho\mathbf{P}\mathbf{S} = \gamma_E\mathbf{I}_n$. Based on Lemma E.1, ED-HNN can solve the optimisation formulated in the right-hand side of Eq. (16) with $\rho > 0$ and $\mathbf{W} = \mathbf{W}_S$.

For PhenomNN (Wang et al., 2023b) formulated as Eq. (13), devoid non-linear activation and by setting the learnable transformation matrix to the identity matrix, we have:

$$\begin{aligned} \mathbf{X}_\nu^{(L)} = & \left[\left((\gamma_0 \mathbf{D}_C + \gamma_1 \mathbf{D}_{\mathcal{H}^\nu} + \mathbf{I}_n)^{-1} \left(\gamma_0 (1 - 2\gamma_2) \mathbf{D}_C + (1 - \gamma_2) (\gamma_1 \mathbf{D}_{\mathcal{H}^\nu} + \mathbf{I}_n) + 2\gamma_2 \gamma_0 \mathbf{W}_C + \gamma_2 \gamma_1 \mathbf{H} \mathbf{D}_{\mathcal{H}^\varepsilon}^{-1} \mathbf{H}^\top \right) \right)^L \right. \\ & \left. + \gamma_2 (\gamma_0 \mathbf{D}_C + \gamma_1 \mathbf{D}_{\mathcal{H}^\nu} + \mathbf{I}_n)^{-1} \sum_{l=0}^{L-1} \left((\gamma_0 \mathbf{D}_C + \gamma_1 \mathbf{D}_{\mathcal{H}^\nu} + \mathbf{I}_n)^{-1} \left(\gamma_0 (1 - 2\gamma_2) \mathbf{D}_C + (1 - \gamma_2) (\gamma_1 \mathbf{D}_{\mathcal{H}^\nu} + \mathbf{I}_n) + 2\gamma_2 \gamma_0 \mathbf{W}_C + \gamma_2 \gamma_1 \mathbf{H} \mathbf{D}_{\mathcal{H}^\varepsilon}^{-1} \mathbf{H}^\top \right) \right)^l \right]. \end{aligned} \quad (29)$$

To make our analysis more accessible, we further simplify Eq. (29) by setting $\gamma_2 = \frac{1}{2}$ and $\tilde{\mathbf{D}}^{-1} = \frac{1}{2}(\gamma_0 \mathbf{D}_C + \gamma_1 \mathbf{D}_{\mathcal{H}^\nu} + \mathbf{I}_n)^{-1}$. Then, an L -layer PhenomNN (Wang et al., 2023b) can be further reformulated as:

$$\mathbf{X}_\nu^{(L)} = \left(\tilde{\mathbf{D}}^{-L} (\lambda_1 \mathbf{D}_{\mathcal{H}^\nu} + \mathbf{I}_n + 2\lambda_0 \mathbf{W}_C + \lambda_1 \mathbf{H} \mathbf{D}_{\mathcal{H}^\varepsilon}^{-1} \mathbf{H}^\top) \right)^L + \sum_{l=0}^{L-1} \tilde{\mathbf{D}}^{-l} (\lambda_1 \mathbf{D}_{\mathcal{H}^\nu} + \mathbf{I}_n + 2\lambda_0 \mathbf{W}_C + \lambda_1 \mathbf{H} \mathbf{D}_{\mathcal{H}^\varepsilon}^{-1} \mathbf{H}^\top)^l \tilde{\mathbf{D}}^{-1} \mathbf{X}_\nu^{(0)}. \quad (30)$$

Based on Lemma E.9, when $L \rightarrow +\infty$, the left term tends to $\mathbf{0}$ and the right term becomes a convergent geometric series (Meyer & Stewart, 2023). Hence we have:

$$\mathbf{X}_\nu^{(+\infty)} = (\mathbf{I}_n - \tilde{\mathbf{D}}^{-1} \mathbf{W}_P)^{-1} \tilde{\mathbf{D}}^{-1} \mathbf{X}_\nu^{(0)}.$$

where $\mathbf{W}_P = \lambda_1 \mathbf{D}_{\mathcal{H}^V} + \mathbf{I}_n + 2\lambda_0 \mathbf{W}_C + \lambda_1 \mathbf{H} \mathbf{D}_{\mathcal{H}^E}^{-1} \mathbf{H}^\top$. Based on Lemma E.3, E.4, and E.9, this formula is a special case of Eq. (17), when $\mathbf{W} = \mathbf{W}_P$, $(\mathbf{D} + \rho \mathbf{P})^{-1} = \tilde{\mathbf{D}}^{-1}$ and $(\mathbf{D} + \rho \mathbf{P})^{-1} \rho \mathbf{P} \mathbf{S} = \tilde{\mathbf{D}}^{-1}$. Based on Lemma E.1, PhenomNN can solve the optimisation formulated in the right-hand side of Eq. (16) with $\rho > 0$ and $\mathbf{W} = \mathbf{W}_P$.

For GNN formulated as Eq. (14), without non-linear activation and by setting the learnable transformation matrix to the identity matrix, we have:

$$\mathbf{X}_V^{(L)} = \left((1 - \beta)^L (\mathbf{W}_N)^L + \beta \sum_{l=0}^{L-1} (1 - \beta)^l (\mathbf{W}_N)^l \right) \mathbf{X}_V^{(0)}.$$

$\alpha \in (0, 1)$ and \mathbf{W}_N is symmetrically normalised, which means $\det(\mathbf{W}_N) \leq 1$. Hence, we have, when $L \rightarrow +\infty$, the left term tends to 0 and the right term becomes a convergent geometric series (Meyer & Stewart, 2023). Therefore we can have:

$$\mathbf{X}_V^{(+\infty)} = \alpha (\mathbf{I}_n - (1 - \alpha) \mathbf{W}_N)^{-1} \mathbf{X}_V^{(0)}.$$

Based on Lemma E.3 and E.4, this formula is a special case of Eq. (17), when $\mathbf{W} = \mathbf{W}_N$, $(\mathbf{D} + \rho \mathbf{P})^{-1} = (1 - \alpha) \mathbf{I}_n$ and $(\mathbf{D} + \rho \mathbf{P})^{-1} \rho \mathbf{P} \mathbf{S} = \alpha \mathbf{I}_n$. Based on Lemma E.1, it can solve the optimisation formulated in the right-hand side of Eq. (16) with $\rho > 0$ and $\mathbf{W} = \mathbf{W}_N$. \square

F. Proof of Proposition 3.3.

Without the non-linear activation, we can reformulate an L -layer GNN including the initial residual connection formulated in Eq. (14) as follows:

$$\mathbf{X}_V^{(L)} = \sum_{l=0}^L \theta_l \mathbf{W}^l \mathbf{X}_V^{(0)} \Theta, \quad (31)$$

where $\Theta \in \mathbb{R}^d$ denotes some learnable parameters, and $\theta_l \in \mathbb{R}$ denotes a learnable parameter.

Then, we restate Proposition 3.3 as follows:

Proposition F.1. Consider a hypergraph $\mathcal{H} = \{\mathcal{V}, \mathcal{E}, \mathbf{H}\}$ and its weighted clique expansion $\mathcal{G} = \{\mathcal{V}, \mathbf{W}\}$. Let $\mathbf{X}_V^{(0)} \in \mathbb{R}^{n \times d}$ represent the initial node features. For any $\mathbf{X}_{\mathcal{H}^V} \in \mathcal{X}_{\mathcal{H}^V}^O$ generated by a HyperGNN on \mathcal{H} , there exists a list $[\theta_0^*, \dots, \theta_L^*]$ and a $\Theta^* \in \mathbb{R}^d$ such that $\mathbf{X}_{\mathcal{H}^V} = \sum_{l=0}^L \theta_l^* \mathbf{W}^l \mathbf{X}_V^{(0)} \Theta^*$, if the following conditions hold:

- All rows of $\mathbf{U}^\top \mathbf{X}_V^{(0)}$ are not zero vectors with $\mathbf{U} \in \mathbb{R}^{n \times n}$ comprising the linearly independent eigenvectors of \mathbf{W} .
- \mathbf{W} has no repeated eigenvalues.

Before proving Proposition F.1, we first prove the following Lemmas.

Lemma F.1. Assuming all rows of $\mathbf{X} \in \mathbb{R}^{n \times d}$ are not zero vectors, we can always find a $\Theta \in \mathbb{R}^d$ such that each row in $\mathbf{X}\Theta$ is not zero.

Proof. Consider the i^{th} row of $\mathbf{X}\Theta$ equals 0. In other words, $\mathbf{X}_i \Theta = 0$. Let the solution space of Θ be Q_i . As $\mathbf{X}_i \neq 0$, Q_i is a proper subspace of \mathbb{R}^d . Therefore, $\mathbb{R}^d - \bigcup_{i=1}^n Q_i \neq \emptyset$. All vectors Θ in $\mathbb{R}^d - \bigcup_{i=1}^n Q_i \neq \emptyset$ can meet the requirements. \square

Lemma F.2. Assuming $\mathbf{W} \in \mathbb{R}^{n \times n}$ is a graph adjacency matrix with no duplicate eigenvalues whose eigendecomposition is $\mathbf{W} = \mathbf{U} \Lambda \mathbf{U}^\top$, $\mathbf{X} \in \mathbb{R}^{n \times d}$, $\Theta \in \mathbb{R}^d$ denotes learnable parameters, and all rows of $\mathbf{U}^\top \mathbf{X} \in \mathbb{R}^{n \times d}$ are not zero vectors, for any $\mathbf{Z} \in \mathbb{R}^n$ there exist a list $[\theta_0, \theta_1, \dots, \theta_{n-1}]$, in which $\theta_l \in \mathbb{R}$ is a learnable parameter, to make:

$$\mathbf{Z} = \sum_{l=0}^{n-1} \theta_l \mathbf{W}^l \mathbf{X} \Theta, \quad (32)$$

Proof. Applying eigendecomposition to \mathbf{W} , we can further reformulate Eq. (32) as:

$$\mathbf{Z} = \sum_{l=0}^{n-1} \theta_l \mathbf{W}^l \mathbf{X} \Theta = \sum_{l=0}^{n-1} \mathbf{U} \theta_l \Lambda^l \mathbf{U}^\top \mathbf{X} \Theta,$$

According to Lemma F.1, we can set $\Theta^* \in \mathbb{R}^d$ as a matrix making all rows of $\mathbf{U}^\top \mathbf{X} \Theta^* \in \mathbb{R}^n$ not zero vectors.

Then we use $\mathbf{U}^\top \mathbf{X}'$, in which $\mathbf{X}' = \mathbf{X}\Theta$, to produce the output. For any one-dimension prediction $\mathbf{Z} \in \mathbb{R}^n$, $\tilde{\mathbf{Z}} = \mathbf{U}^\top \mathbf{Z} \in \mathbb{R}^n$. If there exists a polynomial that $g^*(\Lambda_{ii}) = \mathbf{R}_i$, where \mathbf{R} is a vector whose i^{th} row $\mathbf{R}_i = \frac{\tilde{\mathbf{Z}}_i}{(\mathbf{U}^\top \mathbf{X}')_i}$, for $i \in \{1, 2, \dots, n\}$, the righthand side of Eq. (32) can produce \mathbf{Z} .

As Λ_{ii} are different from each other, consider an $n-1$ degree polynomial, $g(\Lambda_{ii}) = \sum_{k=0}^{n-1} \theta_k \Lambda_{ii}^k$. The coefficient θ_k of g^* is the solution of the linear system $\mathbf{B}\omega = \mathbf{R}$, where $\mathbf{B} \in \mathbb{R}^{n \times n}$ with $\mathbf{B}_{ij} = \Lambda_{ii}^{j-1}$, $\omega \in \mathbb{R}^n$ with $\omega_k = \theta_{k-1}$, and $\mathbf{R} \in \mathbb{R}^n$, gives the coefficient of g . As \mathbf{B}^T is a Vandermonde matrix and becomes nonsingular if eigenvalues are different from each other, a solution always exists. Therefore, the righthand side of Eq. (32) can produce arbitrary one-dimensional vectors. \square

After having these Lemmas, we present the proof of Proposition F.1 as follows:

Proof. Based on assumption 3.1, we have $\mathcal{X}_{\mathcal{H}_{1d}}^O \subseteq \mathbb{R}^n$. Hence, when conditions a) and b) hold, according to Lemma F.2 we have, for any $\mathbf{X}_{\mathcal{H}_V} \in \mathcal{X}_{\mathcal{H}_{1d}}^O$ generated by a HyperGNN on \mathcal{H} , there exists a list $[\theta_0^*, \dots, \theta_L^*]$ and a $\Theta^* \in \mathbb{R}^d$ such that $\mathbf{X}_{\mathcal{H}_V} = \sum_{l=0}^L \theta_l^* \mathbf{W}^l \mathbf{X}_V^{(0)} \Theta^*$. \square

G. Discussion about the usage of the initial residual connection.

In this section, we utilise the theoretical results presented in Section 3 to discuss the importance of the initial residual connection in enhancing the performance of WCE-GNN in the hypergraph node classification task.

From the input side. On the basis of Proposition 3.1, with the initial residual connection, the model continually incorporates initial node features across all layers, as opposed to using them only in the first layer without these connections. Consequently, each layer in the model equipped with the initial residual connection can access and utilise a broader range of input information compared to layers in the model without such connections.

From the output side. Drawing from Proposition 3.2, the incorporation of the initial residual connection is crucial for preserving the information of initial node features, preventing the model from exclusively smoothing node features. Therefore, models equipped with the initial residual connection can potentially prevent the oversmoothing issue and outperform their counterparts lacking these connections.

From the expressivity side. As discussed in Proposition 3.3, the absence of these connections limits the model to the L -th order of the polynomial described in Eq. (31), capturing only low-frequency information. In contrast, when the initial residual connection is present, the model works as an L -order polynomial formulated in Eq. (31) that can preserve multi-frequency input information and can potentially produce arbitrary one-dimensional node features.

H. Discussion about the design of our weighted clique expansion.

To recap, for a given hypergraph $\mathcal{H} = \{\mathcal{V}, \mathcal{E}, \mathbf{H}\}$, the edge weight between v_i and v_j in our weighted clique expansion is defined as:

$$\mathbf{W}_{H_{ij}} = \sum_{k=1}^m \frac{\delta(v_i, v_j, e_k)}{\mathbf{D}_{\mathcal{H}_{kk}^{\mathcal{E}}}}$$

where $\delta(\cdot)$ is a function that returns 1 if e_k connect v_i and v_j and returns 0 otherwise. We summarise the relationship between this edge weight and the probability of nodes v_i and v_j being in the same category as the following Lemma:

Lemma H.1. Let $p_{i,j}$ denote the probability of v_i and v_j having the same label, $p'_{i,j}$ represent the probability of v_i and v_j being connected by a hyperedge that contains only nodes with the same label, and \hat{p}_{e_k} be the probability of e_k containing nodes with different labels. Then, $p_{i,j}$ is positively correlated with $\mathbf{W}_{H_{ij}}$ if the following conditions hold:

- Hyperedges with higher degrees are more likely to connect nodes with different labels, and $\hat{p}_{e_k} = g_1\left(\frac{1}{\mathbf{D}_{\mathcal{H}_{kk}^{\mathcal{E}}}}\right)$, where $g_1(\cdot)$ is a function, for any $x, y > 0$, with $g_1(x) \cdot g_1(y) = g_1(x+y)$, $\frac{dg_1}{dx} < 0$, and $g_1(x) \in (0, 1)$.
- $p_{i,j}$ is positively correlated with $p'_{i,j}$, namely, $p_{i,j} = g_2(p'_{i,j})$, where $g_2(\cdot)$ is a function for any $x > 0$ with $\frac{dg_2}{dx} > 0$ and $g_2(x) \in (0, 1)$.

Proof. According to the pre-defined condition a), we can have:

$$p'_{i,j} = 1 - \prod_{e_k \in \hat{\mathcal{E}}_{v_i, v_j}} \hat{p}_{e_k} = 1 - \prod_{e_k \in \hat{\mathcal{E}}_{v_i, v_j}} g_1\left(\frac{1}{\mathbf{D}_{\mathcal{H}_{kk}}^\varepsilon}\right) = 1 - g_1\left(\sum_{e_k \in \hat{\mathcal{E}}_{v_i, v_j}} \frac{1}{\mathbf{D}_{\mathcal{H}_{kk}}^\varepsilon}\right) = 1 - g_1\left(\sum_{k=1}^m \frac{\delta(v_i, v_j, e_k)}{\mathbf{D}_{\mathcal{H}_{kk}}^\varepsilon}\right) = 1 - g_1(\mathbf{W}_{H_{ij}}), \quad (33)$$

where $\hat{\mathcal{E}}_{v_i, v_j}$ is a set containing hyperedges connecting v_i and v_j . Based on Eq. (33) and the pre-defined condition b) we can have:

$$p_{i,j} = g_2(p'_{i,j}) = g_2(1 - g_1(\mathbf{W}_{H_{ij}})). \quad (34)$$

The derivative of Eq. (34) with respect to $\mathbf{W}_{H_{ij}}$ is:

$$\frac{d p_{i,j}}{d \mathbf{W}_{H_{ij}}} = \frac{d g_2}{d \mathbf{W}_{H_{ij}}} = \frac{d g_2}{d p'_{i,j}} \cdot \frac{d p'_{i,j}}{d g_1} \cdot \frac{d g_1}{d \mathbf{W}_{H_{ij}}} = -1 \cdot \frac{d g_2}{d p'_{i,j}} \cdot \frac{d g_1}{d \mathbf{W}_{H_{ij}}}.$$

On the basis of our pre-defined conditions a) and b), we have $\frac{d g_2}{d p'_{i,j}} > 0$ and $\frac{d g_1}{d \mathbf{W}_{H_{ij}}} < 0$, thereby we have:

$$\frac{d p_{i,j}}{d \mathbf{W}_{H_{ij}}} = -1 \cdot \frac{d g_2}{d p'_{i,j}} \cdot \frac{d g_1}{d \mathbf{W}_{H_{ij}}} > 0.$$

As a result, $p_{i,j}$ is positively correlated with $\mathbf{W}_{H_{ij}}$. □

I. CE homophily score.

We quantify the homophily-level of a hypergraph $\mathcal{H} = \{\mathcal{V}, \mathcal{E}, \mathbf{H}\}$ based on the CE homophily score in Wang et al. (2023a), which is also called as the node homophily in Wei et al. (2022). Mathematically, it is defined as:

$$CE_{Score} = \frac{1}{|\mathcal{V}|} \sum_{v \in \mathcal{V}} \frac{|\{v_i : v_i \in \mathcal{N}_v \wedge \mathbf{y}_{v_i} = \mathbf{y}_v\}|}{|\mathcal{N}_v|},$$

where \mathcal{N}_v denotes a set containing neighbouring nodes of v .